NI

NAS 7-100

Report No. TE82-66

THIRD QUARTERLY PROGRESS REPORT
APPLIED THERMIONIC RESEARCH

Contract 951262

25 January to 25 March 1966

by

S. Kitrilakis
D. Lieb
F. Rufeh
L. van Someren

Prepared for

Jet Propulsion Laboratory
Pasadena, California

RG7-47578

Report No. TE82-66

THIRD QUARTERLY PROGRESS REPORT

APPLIED THERMIONIC RESEARCH

Contract 951262

25 January to 25 March 1965

by

S. Kitrilakis
S. Lieb
F. Rufeh
L. van Someren

Prepared for

Jet Propulsion Laboratory
Pasadena, California

Approved by _S. Kitrilakis_

S. Kitrilakis
Research Manager

TABLE OF CONTENTS

TABLE OF CONTENTS (cont)

LIST OF ILLUSTRATIONS

LIST OF ILLUSTRATIONS (continued)

CHAPTER I

INTRODUCTION AND SUMMARY

The technical effort in this program consists of two tasks. (a) The study of electronegative surface additives with the objective of exploiting their demonstrated potential for improving the performance of thermionic converters. (b) The study of inert gas plasma additives as a means of probing the ignited mode plasma and as a possible barrier to the loss of cesium ions.

The surface additive task has been concerned with CsF because of the exceptionally high, though short-lived, performance obtained with this substance in the previous year of the program. In particular, the main objective of the current program in this area was the stabilization of this performance for indefinite periods of time and its subsequent documentation. The first converter tested with CsF exhibited the "additive effects" anticipated but, just as with previous devices, this effect disappeared after fifty hours of testing. A series of diagnostic testing with this device supplemented with glass tube experiments, mass spectrometry and an extensive literature study of related work, resulted in the collection of a large body of evidence to the effect that water contained in the CsF was responsible for the "additive effects" observed in this work and reported in the literature. The surface additive task was then subdivided into two parallel efforts.

The first was devoted to purifying CsF to the extent necessary to allow the determination of its effect on the work function of tungsten at thermionic temperatures. To accomplish this objective, the background pressure over the CsF crystals and in the test vehicle must be reduced below 10^{-10} torr. A special

metal-ceramic tube was designed and fabricated, capable of achieving this requirement. Work function changes produced by the CsF in this device were about 0.1 eV as opposed to 0.6 eV in previous work. These experiments are proceeding with the documentation of the effects of CsF including measurements of its activation desorption energy. Work under progress is expected to determine the true effects of fluorine and possibly the reasons it does not perform as well as oxygen.

The second effort was devoted to the utilization of the beneficial effects of oxygen. The thermodynamic equilibrium of oxygen in the converter environment was analyzed and the conclusion reached that the O_2 pressure required for coverage was chemically compatible with this environment in the vicinity of the collector. A critical experiment was conducted using Cs_2O as the O_2 source. In this experiment, O_2 was used under steady-state conditions for the first time. The emitter work function and power output of the device closely resembled those of the CsF charged devices. This converter was tested for stability for 130 hours without discernible change. A second converter specifically designed for oxygen additive using a Cu_2O oxygen source has been under test for 150 hours producing consistent and reproducible data. This system in a simple and direct manner can exploit the beneficial effects of oxygen under steady-state equilibrium.

The plasma additive task produced experimental results which were used to test the analytical framework presented in the last quarterly report. These results verified the hypothesis that the saturation portion of the ignited mode is diffusion dominated. The scattering of electrons by argon atoms in the ignited mode plasma was found to be 1/200 of the scattering by cesium atoms at the same pressure.

I-2

To provide a reference for comparison in the evaluation of the ion conservation capabilities of argon, the performance of the etched rhenium emitter was documented through parametric mapping using Cs only. During this quarter, the parametric study was completed and it revealed a two-fold improvement in the performance of etched rhenium over polished rhenium. The parametric mapping of the etched rhenium emitter completed in this quarter revealed that the etching preparation resulted in a two-fold improvement in performance over the polished rhenium. Alternatively, the etched rhenium emitter gives the same performance at twice the spacing required by the polished rhenium emitters. This improvement was anticipated on the basis of emitter work function measurements presented in the First Quarterly Report.

CHAPTER II

CsF SURFACE ADDITIVE

A. CsF ADDITIVE CONVERTER

Testing of CsF additive, tungsten emitter, converter (#5000) described in the First Quarterly Report has been concluded during this quarter. The large, initially reproducible, work function changes observed with variations in additive reservoir temperature could not be repeated. In spite of several soaking periods at high reservoir and low electrode temperatures, only short term spikes of the high work function characteristic appeared and those at very different conditions from the initial data. This behavior is thus similar to that of the previous CsF converters although the effect has lasted somewhat longer in this case.

To provide a better overall picture of the history of this diode (#5000), the time and temperature chart shown in Figure II-1A and II-1B was prepared. On this chart, electrode and reservoir temperatures and emitter operating hours are indicated. Time cold was not recorded but the occurrence is indicated by arrows on the temperature lines. At the top of the figure, the measured work function is indicated by solid lines and values at other times are approximated by the dotted lines.

The initial tests with low additive reservoir temperature, T_A, produced approximately bare tungsten work function values as indicated up to hour 6. The additive temperature was then increased in steps allowing many hours of soaking at each level. Until hour 77 with T_A of 670 °K, the surface remained essentially at the bare value. At this time, a short term effect was observed

II-1

when the emitter temperature was rapidly increased. However, the bare value quickly returned and it was not until a reservoir temperature of 770°K was reached that a long term stable effect was obtained. It was then possible to cycle reproducibly between the bare value of about 4.75 eV at a T_A of less than 730°K and the somewaht T_E-dependent higher values of 5.2 to 5.4 eV at a T_A of 770°K. This cycling covered the period from hour 83 to hour 158. In preparation for the next step increase in additive temperature, the collectors were heated. An increased work function which decayed back to the bare value after 24 hours accompanied the T_C increase.

Upon raising T_A, a temporary work function increase was observed. After six hours, the bare level was approached and remained stable until the tube was cooled down at hour 233. Figure II-2 shows the bare, high, and transient work functions observed. After the decay, at hour 210, the surface remained stable at near the bare work function value and only short transient effects could be obtained by raising T_A by soaking with T_C lower than T_A and then raising T_C, or by raising T_A still further to 910°K. However, the original stable values which occurred at a T_A of 770°K could not be reproduced.

During the tests, a large back current, varying with additive reservoir temperature, was observed and is believed to be due to Cs^+ ions produced by the dissociation of the CsF on the hot emitter surface. Using this current, the presence CsF pressure may be inferred and compared with the expected arrival rate. A chart of reservoir temperature, arrival rate pressure, and flow for CsF was prepared to facilitate these calculations and is shown in Figure II-3. For many runs however, the current was so large and the ions so massive that it was not possible to reach saturation. The current was thus

II-2

space-charge limited except at additive temperatures below 750 °K. Figure II-4 shows an ion J-V characteristic with a saturation current of about 3 mA/cm^2 which corresponds to a T_A of 735 °K. These observations confirm the presence of CsF pressure in the converter even after the additive effect had disappeared.

One implication of the presence of the ion current is that the CsF is being broken down on the emitter surface and cesium is continuously being formed in the test vehicle. Cooling the emitter allows any such cesium to cover the surface and the emitted current will then follow the characteristic Langmuir S-curve as the surface is heated. From the maximum and minimum points on the curve an effective reservoir temperature may be calculated. Figure II-5 shows one such curve with constant heat input. Emitter temperature is therefore, represented by time on the X axis. The calculated reservoir temperature for this plot was 340 to 360 °K and corresponds to a pressure of 10^{-4} to 10^{-5} torr. Some cesium was evidently being consumed in the tube since higher pressures were obtained immediately after heating the emitter, and after a cold period, lower ones. Because of the high T_E/T_R ratio of about 6, the small amount of cesium should not significantly cover the emitter surface and could not account for the loss of CsF effect. Attempts were made to drive the cesium into its reservoir, but no change in behavior was observed.

Cesium was finally admitted to the test vehicle by cracking the metal capsule in its reservoir. Since the cesium pressure could then be controlled from its reservoir, any unexpected changes produced by the small amount of free Cs previously present could be eliminated. Work function values obtained are plotted versus T_E/T_R in Figure II-6 and show the "untreated tungsten" characteristic obtained in earlier work with tube #1000 and tube #3000 after a period of testing. Loss of additive effect with CsF-only in the converter directly

II-3

corresponds to loss of additive effect when Cs is also present. Together with the covered work function calculations described in the second quarterly, these results show that the CsF-only experiments form a valid basis for converter behavior predictions.

While this particular device has not been disassembled, autopsy and analysis of the earlier converters has shown[1] that even after the irreversible loss of additive effect CsF pellets are still present in the device, in one case almost in their original form.

The results obtained from these converter studies may be summarized as follows:

1. There is an apparent threshold in additive effect; stable effects do not appear until a certain additive reservoir temperature is reached, usually about 700°K.

2. Only two stable work function levels have been observed, a bare at about 4.8 eV and an additive at about 5.3 to 5.5 eV.

3. When a high CsF reservoir temperature is used together with a high emitter temperature the work function values soon decay to the bare level and a permanent degradation occurs.

After degradation:

1. CsF is still present in the device with a pressure responsive to its reservoir temperature.

65-R-12-106
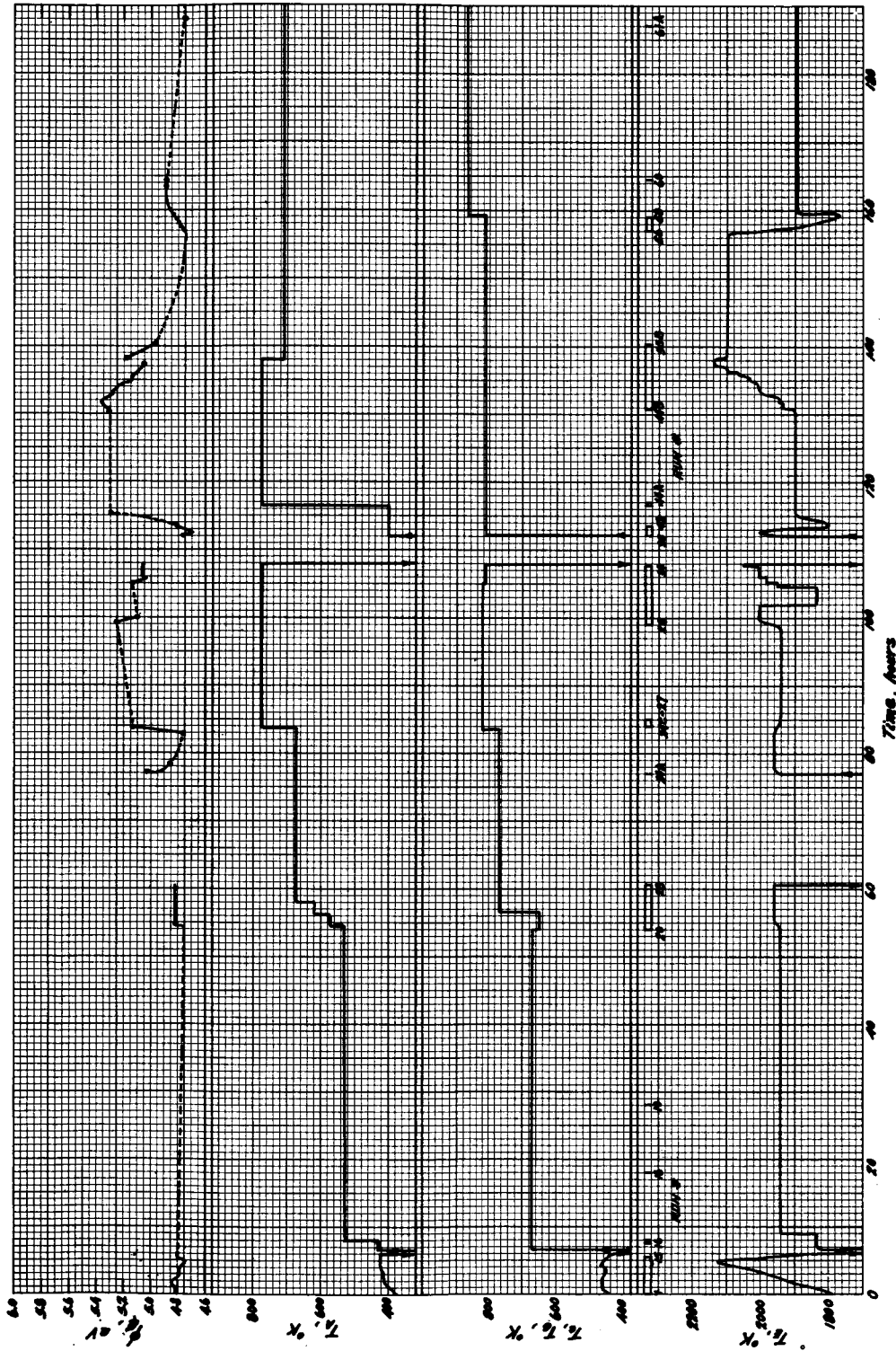
Figure II-1A. Time, Temperature and Work Function.
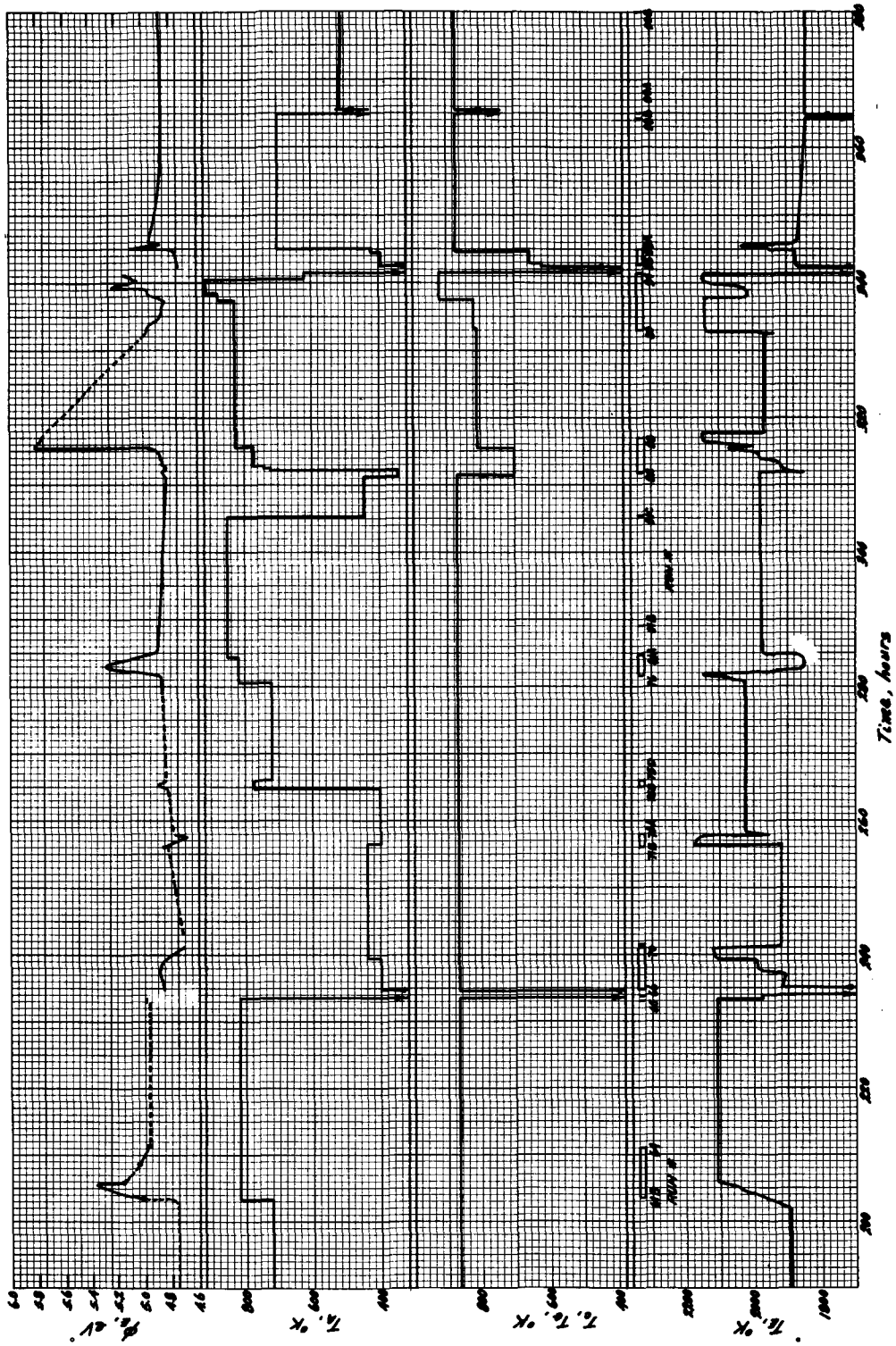
Figure II-1B. History of CsF Converter (5000).
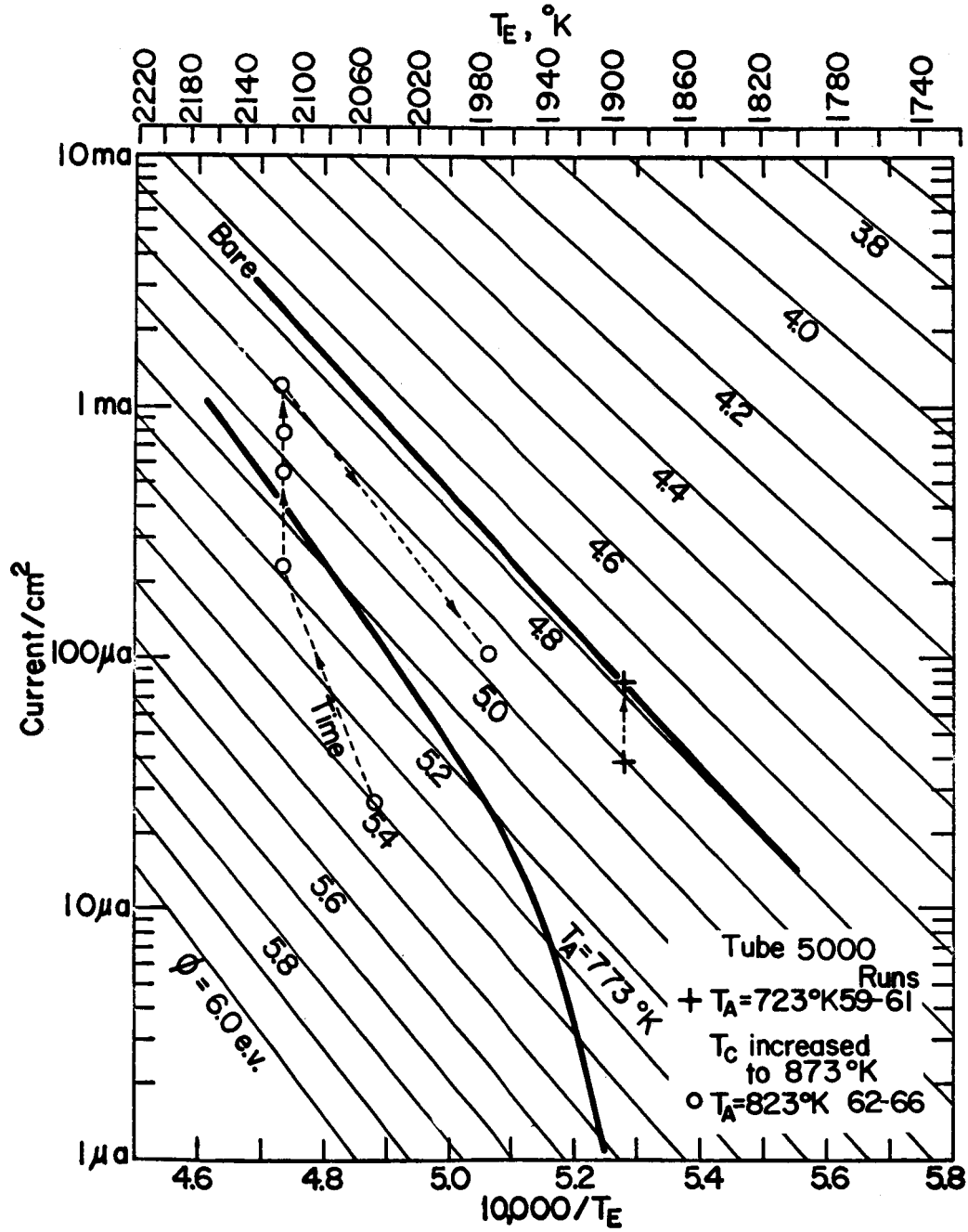
Figure II-2. CsF Only Work Functions in Converter #5000.
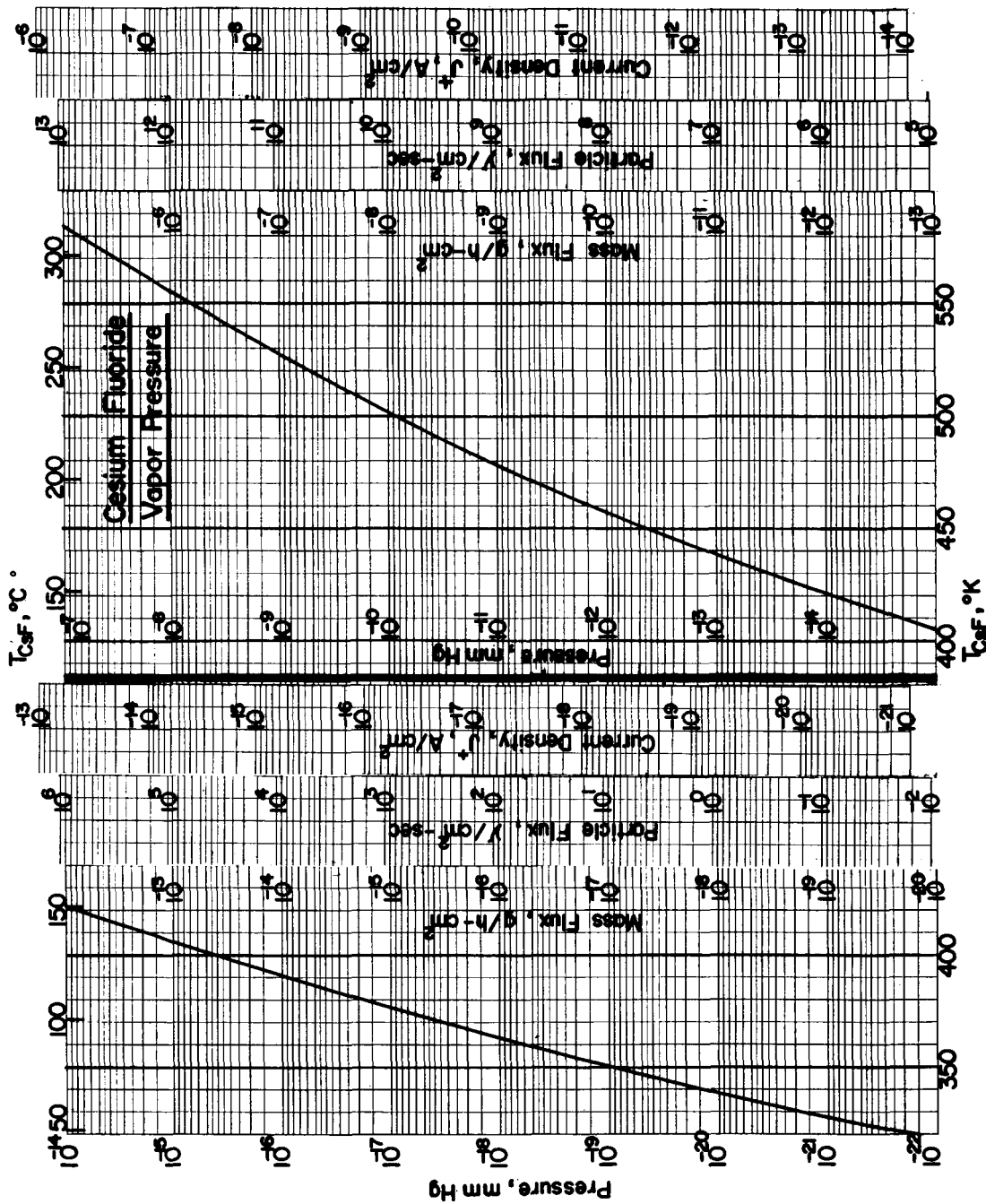
Figure II-3. CsF Arrival Rate as a Function of Temperature
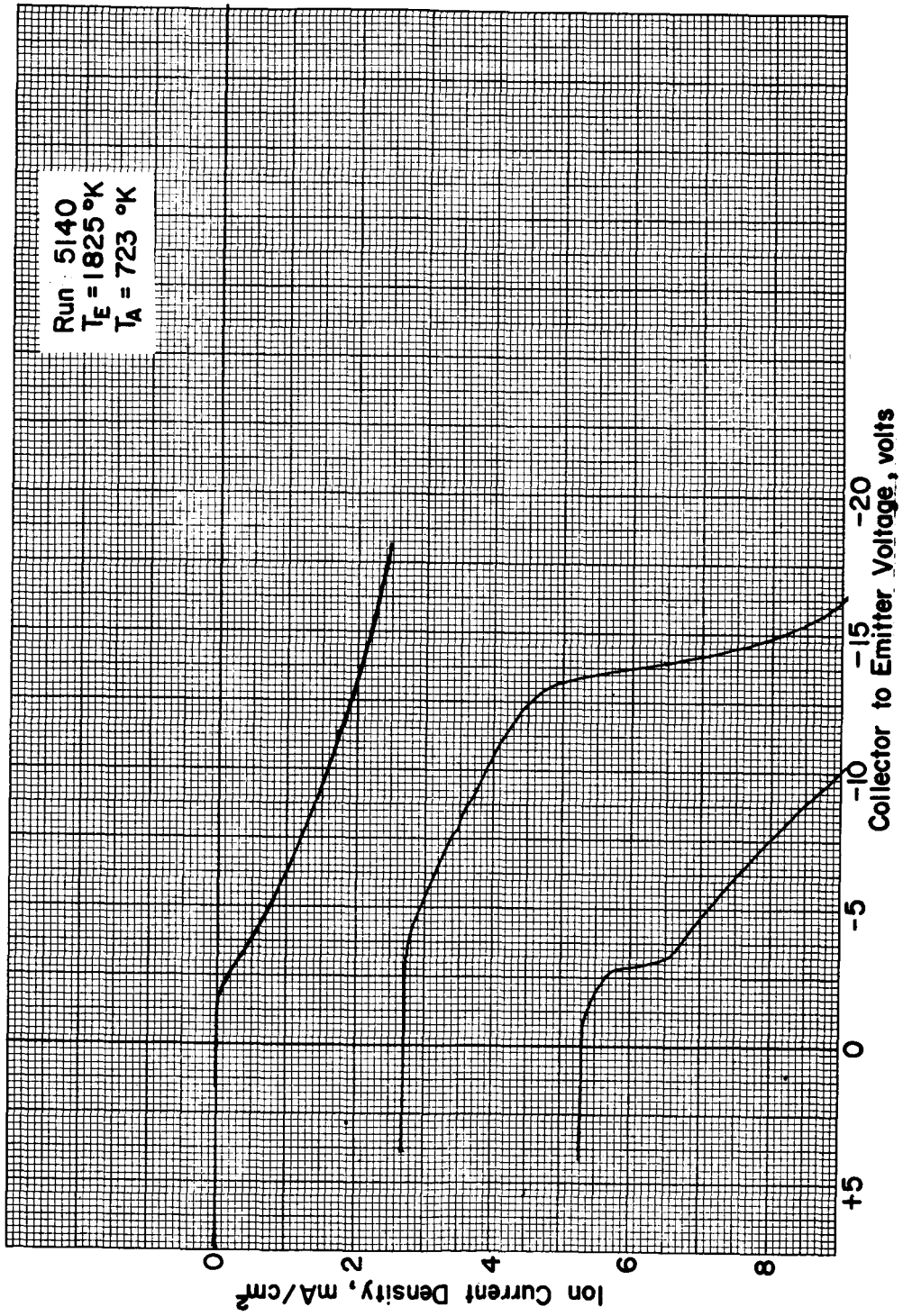
Figure II-4. Cs⁺ Ion Current Showing Space Charge Limiting.

Run 5140
$T_E = 1825\,°K$
$T_A = 723\,°K$

Collector to Emitter Voltage, volts

Ion Current Density, mA/cm²
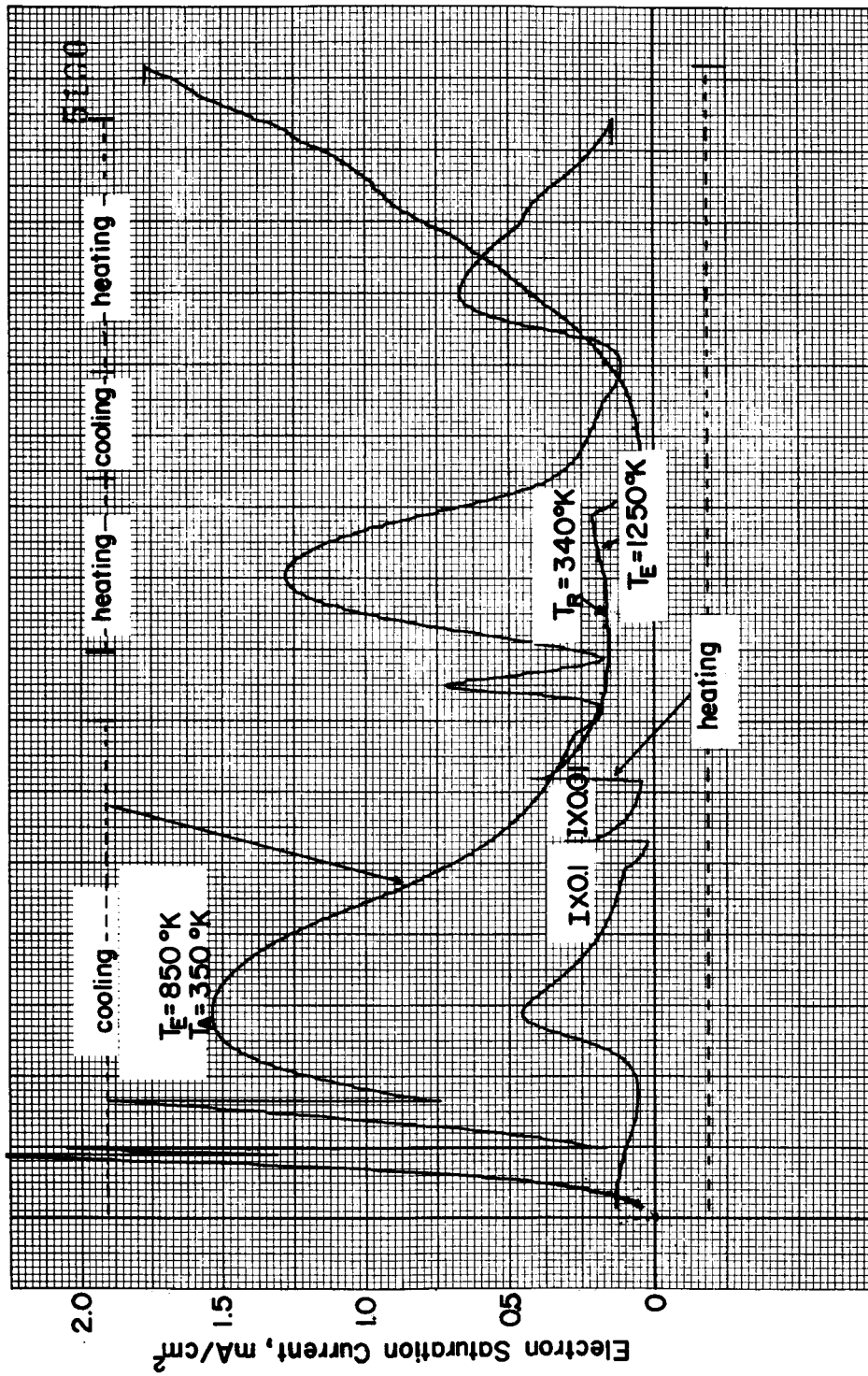
Figure II-5.   Electron Current Peaks Due to Heating and Cooling of the Emitter.
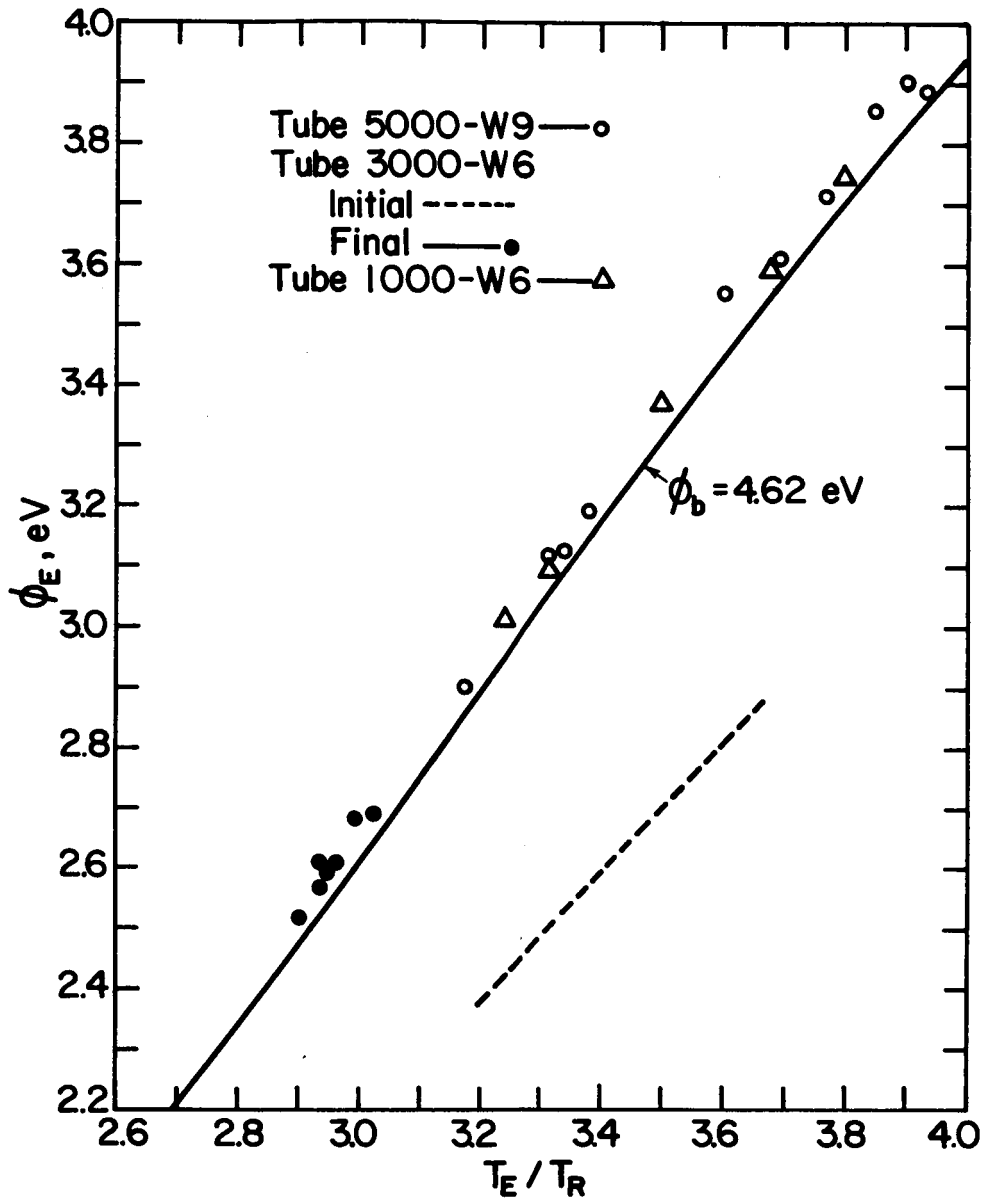
Figure II-6. Comparison of Cesiated ϕ for Various CsF Converters.

2. Conditions favoring abnormally high additive coverage, such as low emitter temperature, soaking or raising of collector temperature, produce a short transient increase in work function.

3. Very high additive reservoir temperatures do not produce significant changes in work function beyond a short transient.

Two possibilities for the loss of additive effect may be proposed at this point, either there is a contaminating substance introduced along with the CsF pellets or else the test vehicle emitter becomes "poisoned" and unresponsive to CsF vapor. Since experiments with complete converters are quite complex and time consuming another testing system capable of determining the causes of the phenomena just discussed was devised.

B. CsF ADDITIVE DIAGNOSTIC STUDY

1. General

A multiple approach aimed at separating the problems of transport and "poisoning" from those of contaminants was adopted. A number of wire-filament glass-envelope tubes in which it was possible to perform many "additive-only" experiments quickly and cheaply were used for work function evaluations. At the same time, the outgassing of CsF pellets was studied using both an ion pump and a mass spectrometer. A detailed study of the literature was also undertaken to more carefully examine the outgassing schedules, techniques and results of other investigators. These topics are discussed briefly below and in more detail in the Appendix.

2. Glass Tube Design

The glass tube design adopted consisted of a 0.005" tungsten-filament-emitter mounted opposite a molybdenum-ribbon-collector. CsF or other additives were placed in the glass envelope and the pressure was regulated by controlling the envelope temperature. In effect, the tungsten "emitter" was located within the additive reservoir. Thus, the glass tube experiment was expected to eliminate the possibility of poor communication of the reservoir with the emitter surface and allow direct investigation of the possibilities of impurities and of chemical reactions of additives with the converter components. Figure II-7 shows a picture of a typical filament and collector assembly mounted on a glass press before sealing into the envelope.

3. Experimental Procedure

The tube was outgassed by baking at 200-400 °C in an oven and flashing the tungsten-filament emitter to 2400 °K. After 5 to 6 hours of outgassing, the tube was pinched off and J-V curves generated at various emitter and wall or "reservoir" temperatures. The emitter temperature was measured with an optical pyrometer. A typical J-V curve is shown in Figure II-8. It should be noted that due to the large spacing (about 0.060") and the fact that the filament is directly heated by dc current, about 10 volts have to be applied before the emitter current saturates. This type of heating results in a variation in potential along the filament length and, since the voltage drop is about two volts, the exponential portion of the J-V curve is broadened by the two volts. Neither of the above effects has any influence on the saturation current which is of interest here.
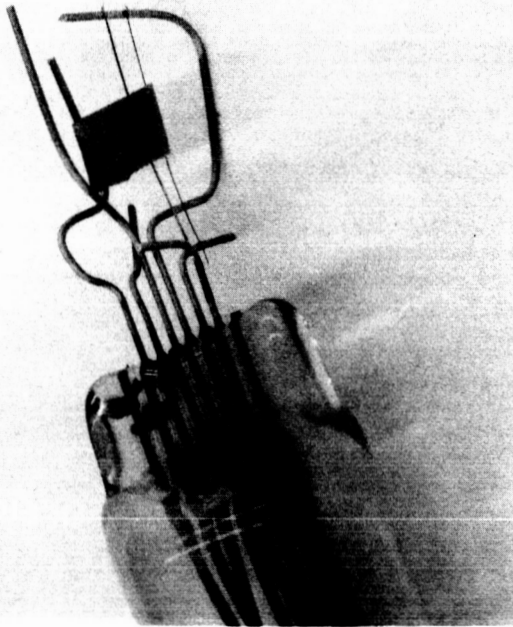
Figure II-7.   Typical Glass Tube Press With Electrodes.
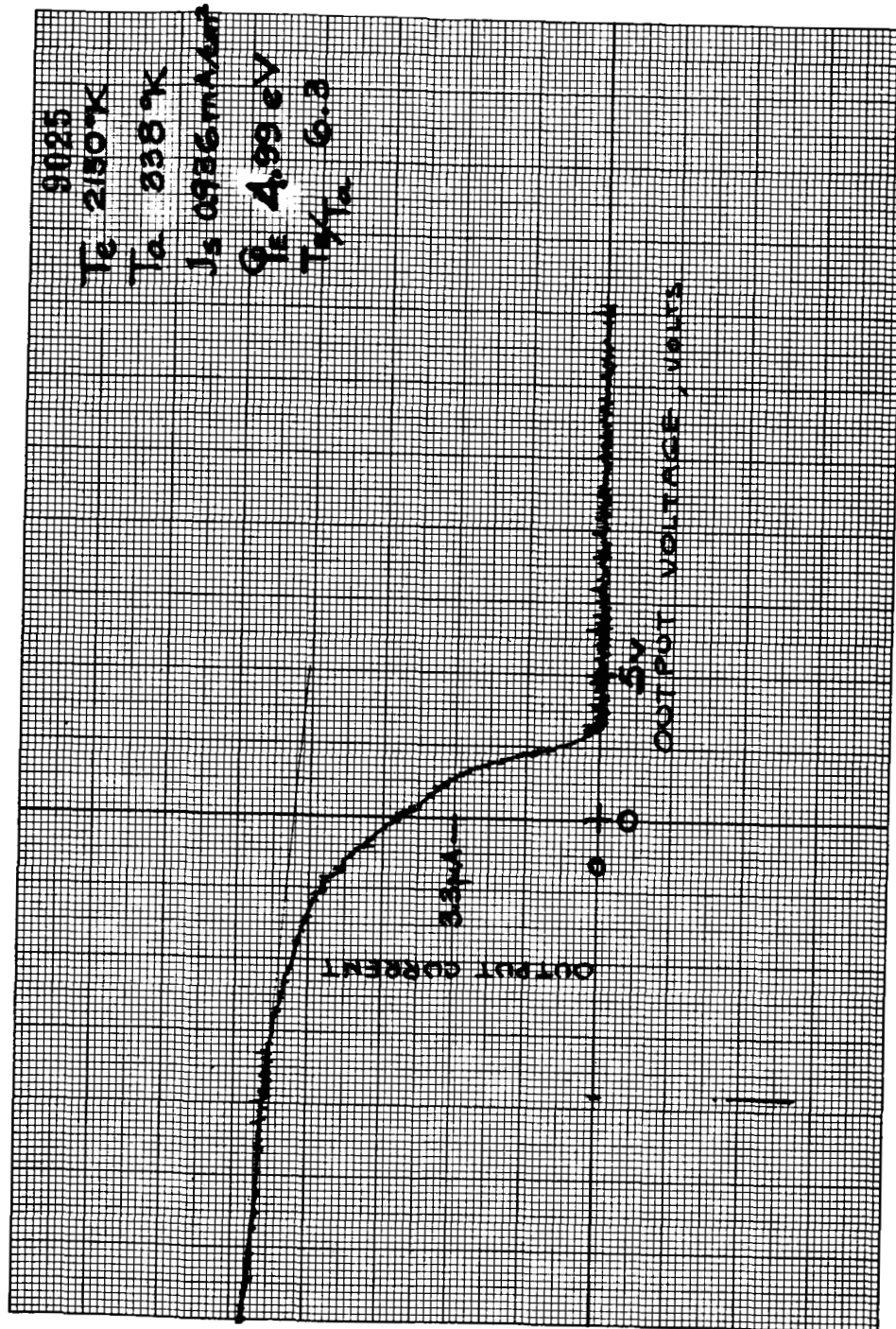
Figure II-8. Typical Glass Tube J-V Characteristic.

From the measured saturation currents work function values were computed using the Richardson equation. The emitting area is, of course, a source of ambiguity. It was estimated by observing pyrometrically the filament and determining the length at high temperature. The area thus obtained was consistent with the emission current for bare tungsten. At any rate, an error of as much as 0.15 to 0.2 V is possible, and the absolute value of work function obtained should not be considered any more accurate than that. On the other hand, the relative values are self-consistent within much narrower limits.

4. Experimental Results

The first tests were performed on a CsF additive tube at emitter temperatures from 2100°K to 2400°K and envelope temperatures from 310°K to 710°K. Figure II-9 is a plot of computed work function versus envelope temperature with 2140°K emitter temperature. A pronounced work function maximum can be seen at about 450°K, in spite of the scatter of $\pm$ 0.1 eV in these measurements. The CsF pressure corresponding to this temperature, as obtained from Figure II-3, is less than 10^{-10} torr and at 670°K it is about 1.5 x 10^{-5} torr.

This tube (9000) showed additive effects at surprisingly low envelope temperatures and indicated an optimum temperature for maximum effect. At the higher envelope temperatures the filaments began to be attacked chemically and finally failed. The second tube ('1000) produced similar results and at the conclusion of these runs the glass envelope near the filament region, was coated with a metallic deposit, apparently tungsten from the filaments. Considering the low filament temperatures (1800-2100°K) used, evaporation was not a

reasonable explanation and some sort of chemical erosion must have been taking place. Figure II-10 shows comparision micrographs of the filament from tube 9000 and a purposely evaporated (2800 °K) test filament. The definite pitting observed on the tube filament as compared to the control in Figure II-10 shows that there must be processes other than evaporation taking place. The arrival rate curve of Figure II-3 shows that at the low temperatures (80-300 °C) used, it is highly unlikely that the CsF could cause the observed chemical attack and pronounced work function shift. For example, at 300 °C the CsF arrival rate is about 4×10^{12} particles/cm^2 sec. and at this rate, it would take 2.5×10^2 sec. to form a monolayer consisting of 10^{15} atoms/cm^2. At 80 °C with the arrival rate of 10 particles/cm^2-sec. a monolayer would never form during the experiment. It is reasonable to assume that a coverage which is at least 10% of monolayer would be required to cause any work function change and therefore, the CsF cannot be responsible for the observed work function change occurring at low envelope temperature.

The maximum possible rate of chemical attack on the filament is limited to the rate of formation of a monolayer, thus in the case of CsF at 300 °C, the filament could lose a maximum 15 monolayers per hour and it would take about 15×10^4 hours to eat through the filament assuming a monolayer is of the order of 3A° thick. Furthermore, tungsten fluoride compounds break down at high temperatures to leave plain tungsten and this system is in fact, customarily used in the chemical vapor deposition of tungsten. In view of the above considerations, the thinning of the filament and the low envelope temperature work function changes are almost certainly due to impurities present either in the glass bulbs or the CsF crystals.
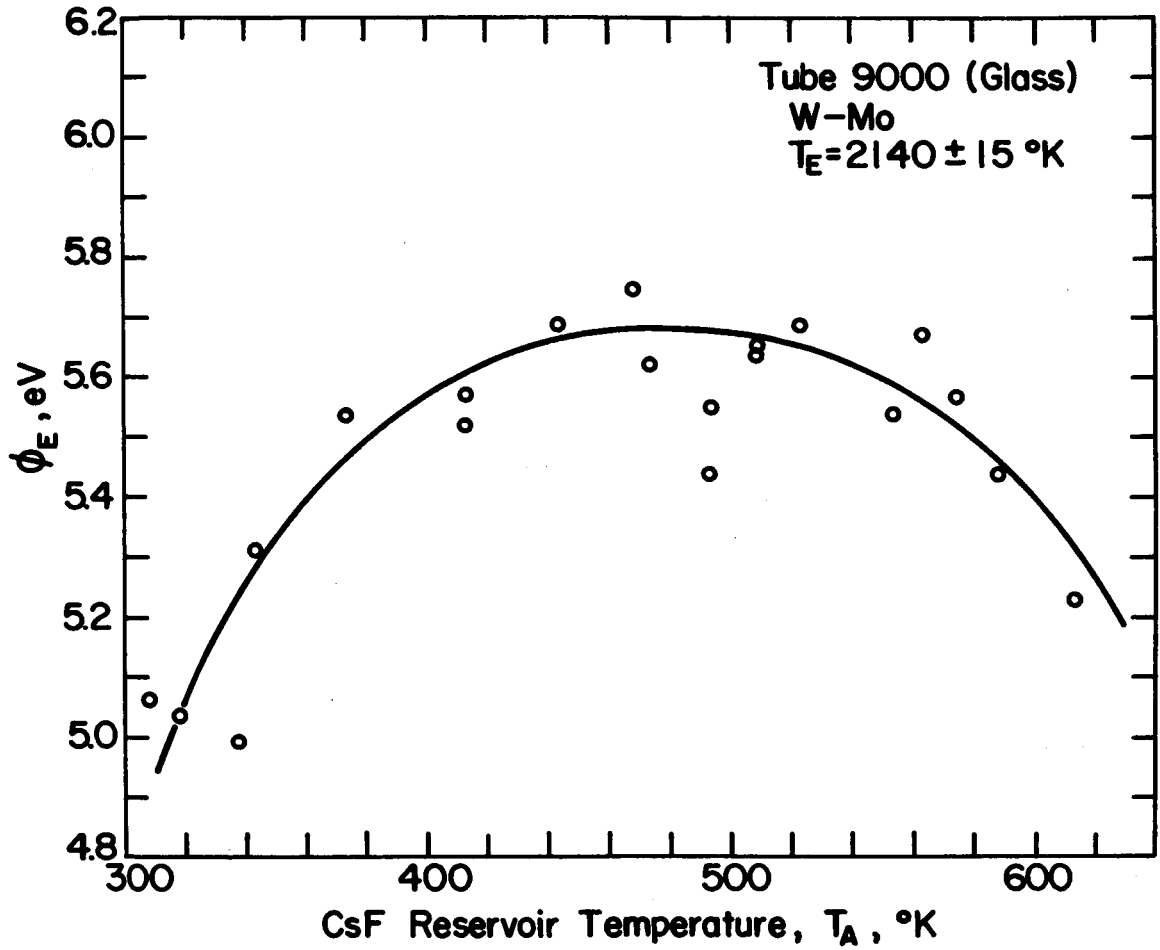
Figure II-9. Work Function Change Produced in CsF Glass Tube.

66-R-1-3
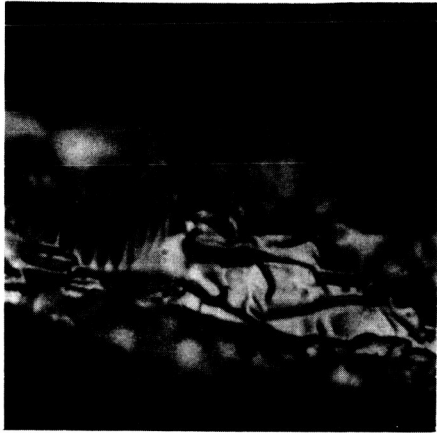
66-R-1-4

Figure II-10A, II-10B. Micro-Photograph of Tungsten Filament Eroded in a Glass Tube.

66-R-1-5
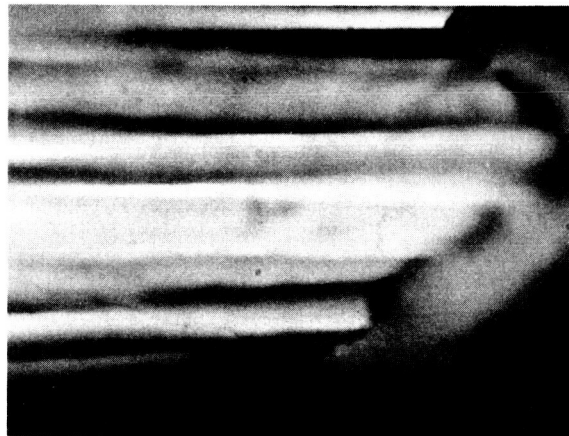
Figure II-10C. Micro-Photograph of Tungsten Filament Operated at High Temperature in Vacuum.

Three additional glass tube experiments were carried out; a CsI tube (12,000) to determine whether a less reactive halide would slow the attack but still produce the desired work function effects, a no-additive control tube (13,000) and a high temperature (500-600°C) outgassed CsF tube (14,000). A rhenium filament was also tried, but was attacked so rapidly, no measurements could be made. Essentially, the same results were obtained in the three devices as in the previous ones, showing that both the erosion and the work function effects were not due to the intentional additives at all but to a contaminant present in the glass as well as in the fluoride. The most likely substance is water since both glass and fluoride contain large quantities of it.

5. Outgassing Experiments

Using an ion pump connected to a pinched-off copper tube, a charge of CsF was heated and the pressure, time, and temperature characteristics examined. It was found that up to 400°C large amounts of gas were evolved which after a period of a few hours decayed. However, when the temperature was further increased to 500°C, additional gas was still present.

6. Mass Spectrometer Analysis

The results of the CsF outgassing experiment outlined above and the experience with the glass tubes precipitated the decision to perform a mass-spectrometric analysis on a sample of CsF. The sample was placed in a vacuum-fired low carbon nickel tube, one end of which was closed while the other end was connected to the mass spectrometer system. A heater was placed around the CsF container and the entire system exhausted. The temperature of the sample was raised and again rapid gas evolution was observed, much too rapid to allow any analysis. After an overnight bake at 100°C the

pressure was found to be steady and low enough to analyze In Figure II-11, the partial pressures of the gases detected are plotted versus time. The left-hand scale corresponds to the partial pressure of each gas in the CsF container. The pressures gradually decay after each increase in baking temperature, but even after 15 hours at 450 °C to 550 °C when the temperature is increased, there is still 10^{-5} torr of CO and 10^{-6} torr of H_2O. This agrees with the results of the ion pump experiment and furthermore, shows that all of the fluoride outgassing schedules used in both the converters and the glass tubes have been inadequate and sufficient water remained in the devices to account for the observed work function changes.

7. Conclusions

Reviewing the past experience with additive converters, together with the above results in the glass tubes and in mass spectrometer experiments, leads to the conclusion that the effects produced were due to water introduced with the fluoride. In the metal devices, this water slowly reacted causing the additive effect to disappear. Furthermore, the literature survey has pointed out that almost all past investigations used CsF not sufficiently outgassed to remove the water. It also becomes obvious that extreme care must be used in any of these investigations to exclude oxygen, since as little as 10^{-8} torr is sufficient to cause a pronounced work function shift. In normal cesiated converters, these effects are not observed since the cesium quickly getters the limited amounts of oxygen present.

C. SURFACES STUDIES WITH PURIFIED CsF

The experience discussed in the previous section made it clear that much more elaborate control of the test vehicle atmosphere is necessary in order to isolate and measure the effects of CsF on the emitter surface. In the course

of a two day meeting among JPL and TEECO representatives, the decision was reached that CsF experiments would continue in a new test vehicle. The new test vehicle employed fabrication and testing techniques capable of reducing residual gas content to extremely low values, i.e., 10^{-11} torr. This section gives a detailed description of the device and experimental procedures.

1. Test Vehicle Design and Assembly

The test vehicle shown in Figure II-12 incorporates two filaments (15) with springs (16) maintaining the tension required to avoid sagging. Lead-throughs provide connections for heating current and emission measurements. The shell (4-6), and (17) provides guarding for the active collector (8). Ceramic rings (7) electrically isolate the sections. The entire shell can be immersed in liquid nitrogen to aid in obtaining contamination free results. Flange (19) connects to a getter ion pump allowing the tube to be pumped continuously during testing. The CsF reservoir (11) is heated electrically by passing a current through its shell. An orifice (14) is arranged to form a beam of CsF molecules which will deposit on the filaments in the region of the collector.

Assembly of the tube is accomplished by first brazing together the shells, flange, and upper leadthroughs. The filament with attached springs is welded to leadthroughs (18). The additive tubulation is welded into place at the outer edge of tube (21) and remains connected to its own ion pump until it is pinched off after outgassing.

During testing, pressure in the tube is monitored by the ion pump current and, because of the close coupling, the readings should be an accurate representation of the actual tube pressure. This measurement will be limited

by the pump leadthrough leakage current which may be estimated under actual vacuum conditions by removing the pump magnet and determining the residual current.

2. Filaments

The filaments are constructed of 0.005" diameter tungsten wire and are about 6 inches in length. Since the filaments are not visible in operation, their temperature is interred from the heating power input. Using the Langmuir-Jones[1] relations for a tungsten filament 0.005" in diameter, Figure II-13 was plotted giving filament temperature as a function of heating current. This relation assumes no gas cooling and an accurate knowledge of the wire diameter.

Non-uniformity in the temperature may arise because of end cooling effects. From the Langmuir MacLane and Blodgett[2] calculations, a plot of distance from the end connection for 99.9% of maximum temperature versus temperature can be made. This plot is also shown in Figure II-13 and assumes that the lead connection is at room temperature. It is seen that lead influence extends less than 0.5 cm from the connection for all temperatures. Clearly, the temperature will be uniform in the collector region.

3. Outgassing

The entire tube assembly with its ion pumps was mounted in a vacuum enclosure during this process to avoid oxidation of the envelope. Pumping was continued until a final pressure of 5×10^{-10} torr was attained when the fluoride pump was pinched off.

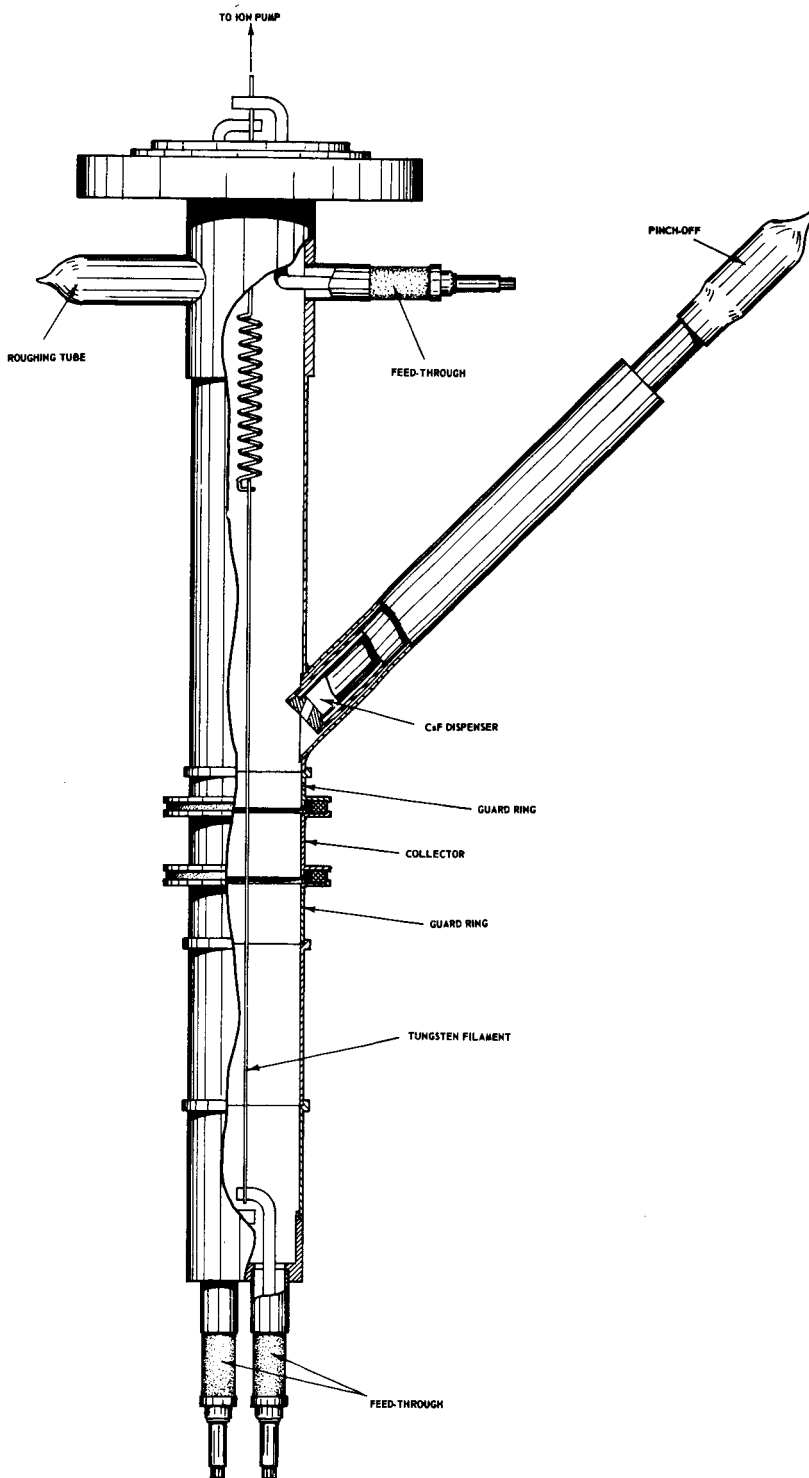Figure II-11. Mass Spectrometer Analysis of CsF Outgassing.

66-R-4-96

Figure II-12. Drawing of Surface Studies Device.
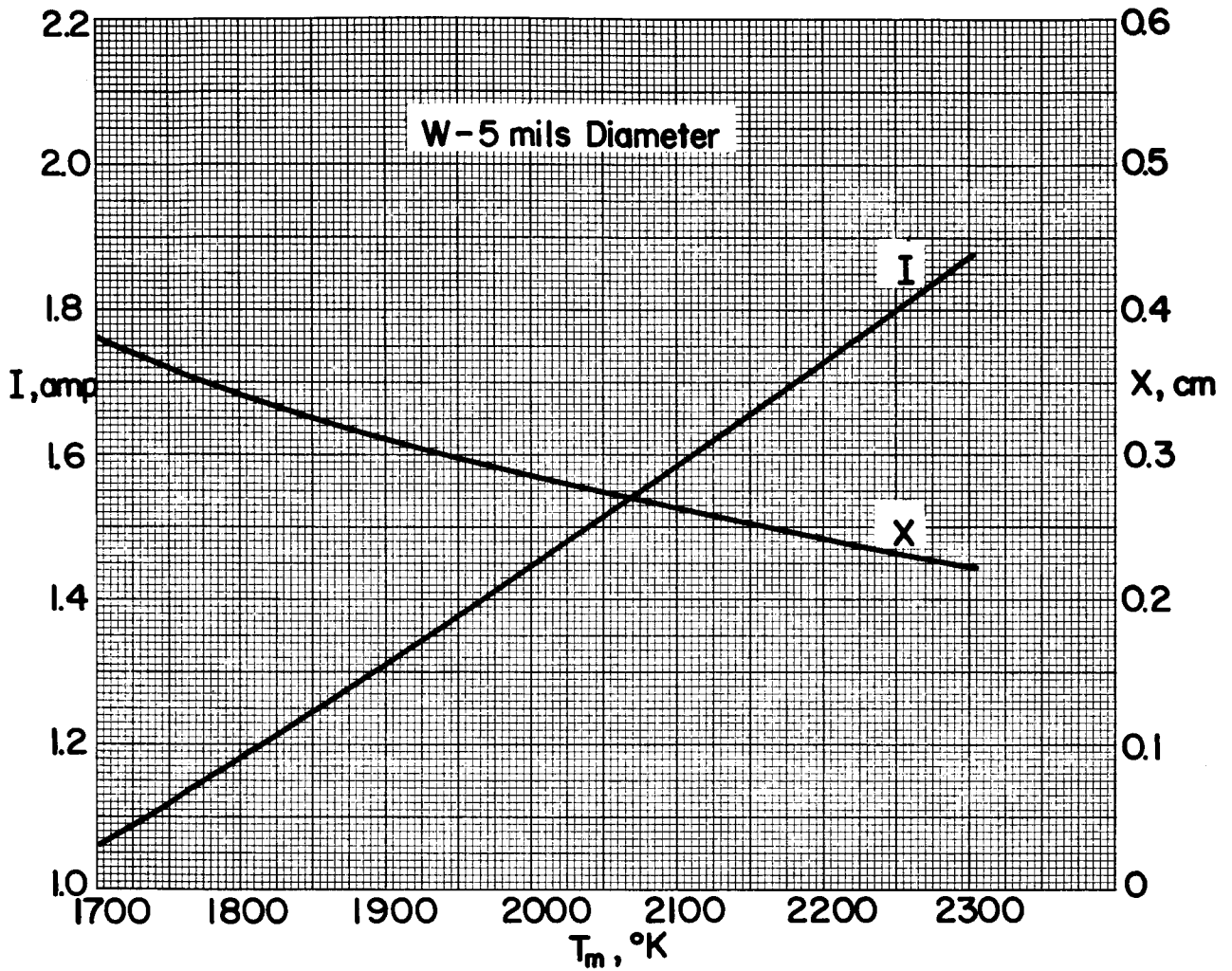
Figure II-13. Heating Current and Uniformity as a Function of Filament Mid Point Temperature

Figure II-14 is a schematic of the outgassing arrangement. The CsF is contained in the trap formed by the "U" bend in its tubulation and may be heated and pumped separately from the test vehicle body. Most of the gases given off were therefore, rapidly exhausted without entering and contaminating the actual test vehicle or its pump. Since cesium fluoride normally contains large quantities of water which are difficult to remove, previously baked fluoride obtained from the outgassing and mass-spectrometer experiments described above was used to charge the test vehicle. A glove-bag with a dry nitrogen ambient reduced water pickup during this charging procedure. Dry nitrogen was also forced through the test vehicle until the additive ion pump was attached, again minimizing possible water and carbon dioxide absorbtion.

The device was then rough pumped through the roughing tubulation. After the pressure was low enough to start the ion pumps and their operation appeared stable, this tubulation was pinched off. Pumping was continued with the device at room temperature until a pressure on the order of 10^{-7} torr was reached. The enclosure was then evacuated and heat applied to the test vehicle to raise its temperature until a pressure of 3×10^{-6} torr was reached at about 200 °C. When the pressure rise had leveled off, the additive tubulation was heated but maintained at a lower temperature. A slowly rising pressure only remotely responsive to temperature appeared after a short time. This was traced to heating of the ion pumps by direct conduction through the flanges in the absence of convective cooling with the vacuum environment. Water cooling was provided for both pumps and heating continued. The tube itself was finally maintained at 500 °C for 18 hours and the fluoride at 300 °C for 17 hours. The fluoride was raised to 500 °C for 1/2 hour preceding the final bake but at this level the evaporation rate becomes significant and to avoid excessive loss, the

temperature was reduced. The tube pressure when hot was 10^{-7} torr which dropped to 5×10^{-10} torr upon cooling. This was considered a satisfactory value and the additive pump was sealed off and the test vehicle removed from the vacuum enclosure. Pressure was monitored by means of the pump current after correcting for leakage as described above. The leakage proved to be less than 10^{-9} Amp making pressure measurements to 10^{-11} torr feasible.

4. Work Function Experiments

Surface work function was calculated, using the Richardson equation from measurements of emitted current at specific surface temperatures. Since the accuracy of the result is dependent on the current density, both area and emitted current must be well defined. The guard structure used in the device eliminates leakage currents and at the same time provides a precise active filament length for use in the calculation of area. Filament temperature, since direct observation is not possible, is determined from the Langmuir tables using filament heating current. A diagram of the electrical circuit used in these tests is shown in Figure II-15. The precision voltmeter is necessary because of the strong dependence of temperature on current. The electrometer ammeter as well as measuring collector current has provision for a low impedance guarding circuit and provides the required following action for the guard electrodes. The output I-V curves are plotted on the x-y recorder providing a complete graph of the characteristics from which saturation currents and contact potentials may be determined.

The completed test vehicle, after outgassing, was inverted in such a manner that the CsF pellets fell into the pinch off rather than down into the tube itself. The objective was to evaluate the bare values before admitting

additives, thereby furnishing a control. Initially, the filaments were cycled several times to about 2000°K and soaked at this temperature for about an hour. This treatment further outgassed the device by cleaning the filaments. The preliminary runs without liquid nitrogen, showing approximately the expected tungsten values of about 4. 7 eV are plotted in Figure II-16. Note that the plot is parallel to the work function lines indicating there is no temperature dependence. These results give confidence to the assumption that the surfaces are clean and nothing significant is being evaporated at the higher temperatures. Near the saturation knee an unusual bump appeared in the curves. With different fila-ment polarity the character would change and become a smooth decrease. The effect is unexplained at present, but may be connected with the pump magnetic field.

The test vehicle was then immersed in liquid nitrogen for further testing. Figure II-17 shows the plots of these results. Only a small change has been pro-duced by flashing the filament 2600°K for five minutes between runs. The pres-sure during the flashing rose to 5×10^{-8} torr and then recovered to about 10^{-9} torr during the run. A control run using both a hot and cold filament was made by heating the additive reservoir but not the tubulation. No change in the char-acteristics of either filament were observed, indicating that heating of the empty CsF reservoir had no effect on the emission. These experiments completed the control evaluation of the test vehicle.

Dismounting and tipping the test vehicle so that the CsF pellets fell from their trap, in the tubulation bend, down into the reservoir, prepared for ad-ditive tests. The pellets could be heard dropping into place and their presence thereby verified.

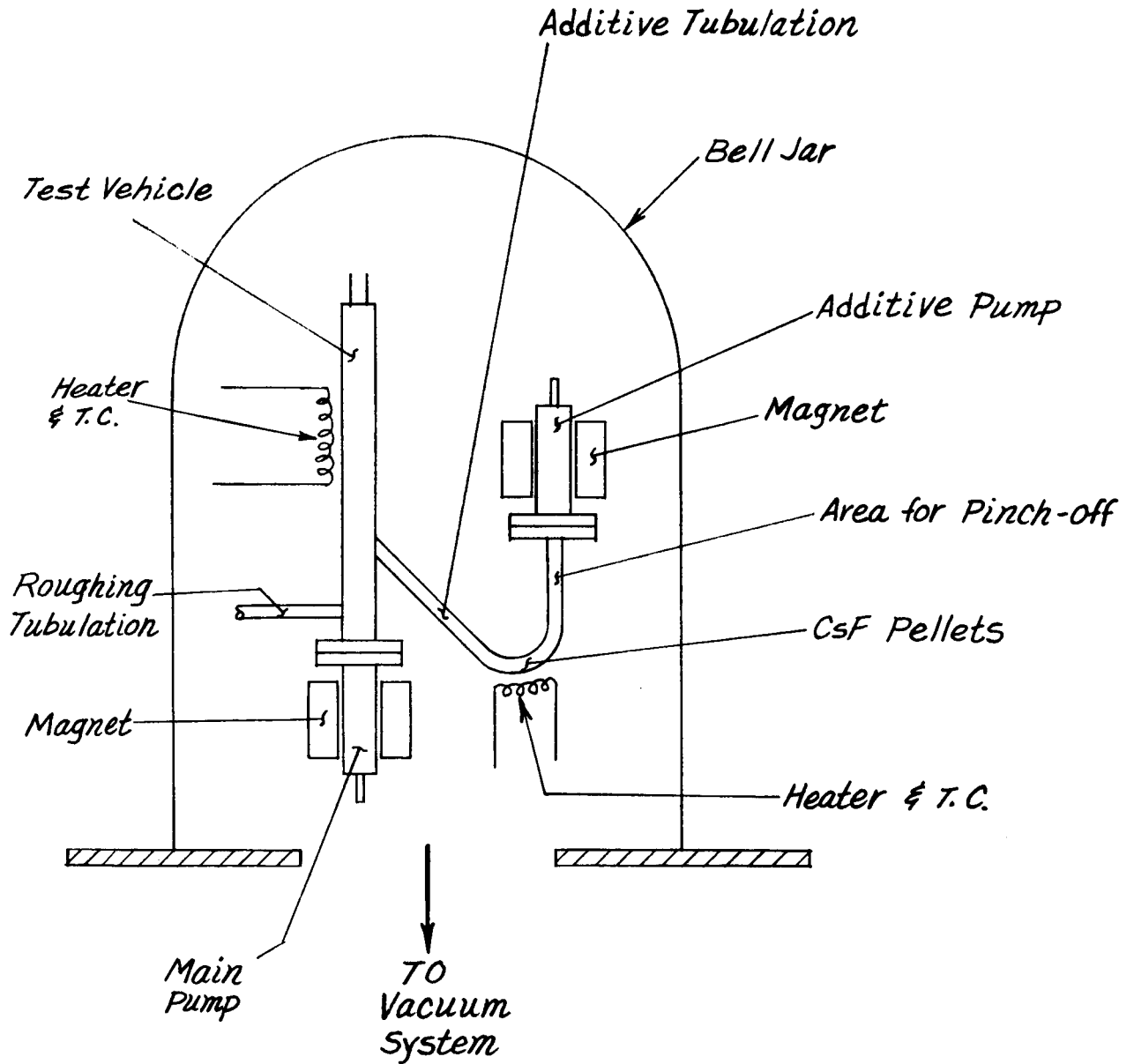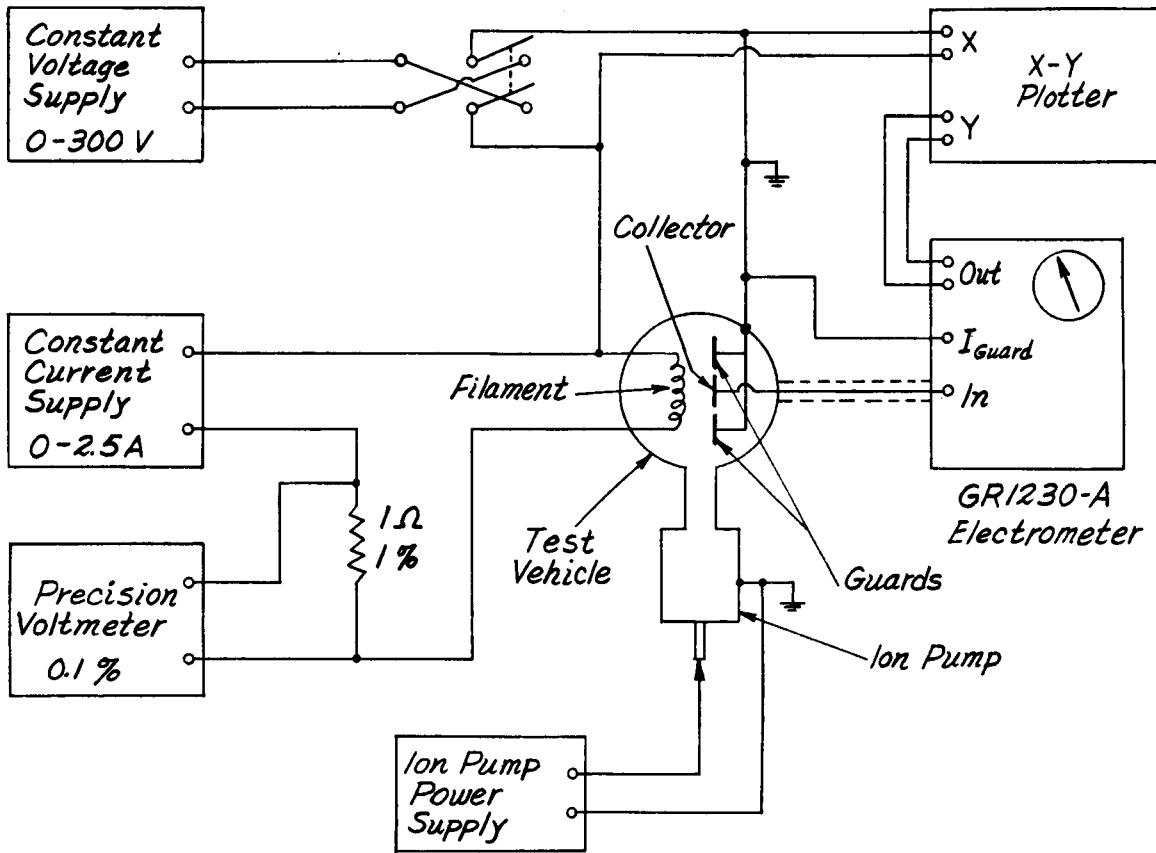Figure II-14.   Outgassing Set-up for Surface Studies Device
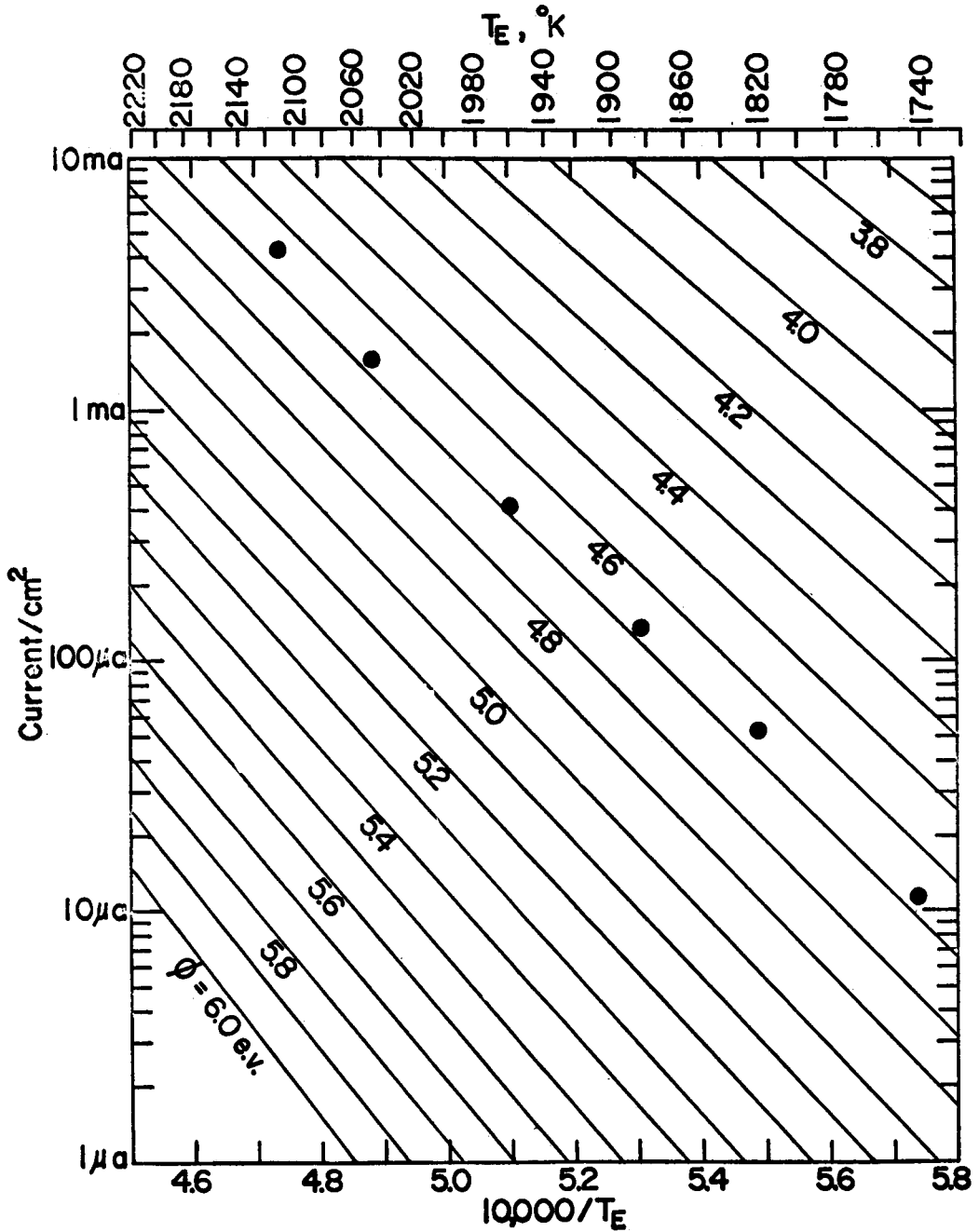
Figure II-15. Circuit Diagram for Emission Measurements

Figure II-16. Work Function for Left Filament and No Liquid Nitrogen Cooling
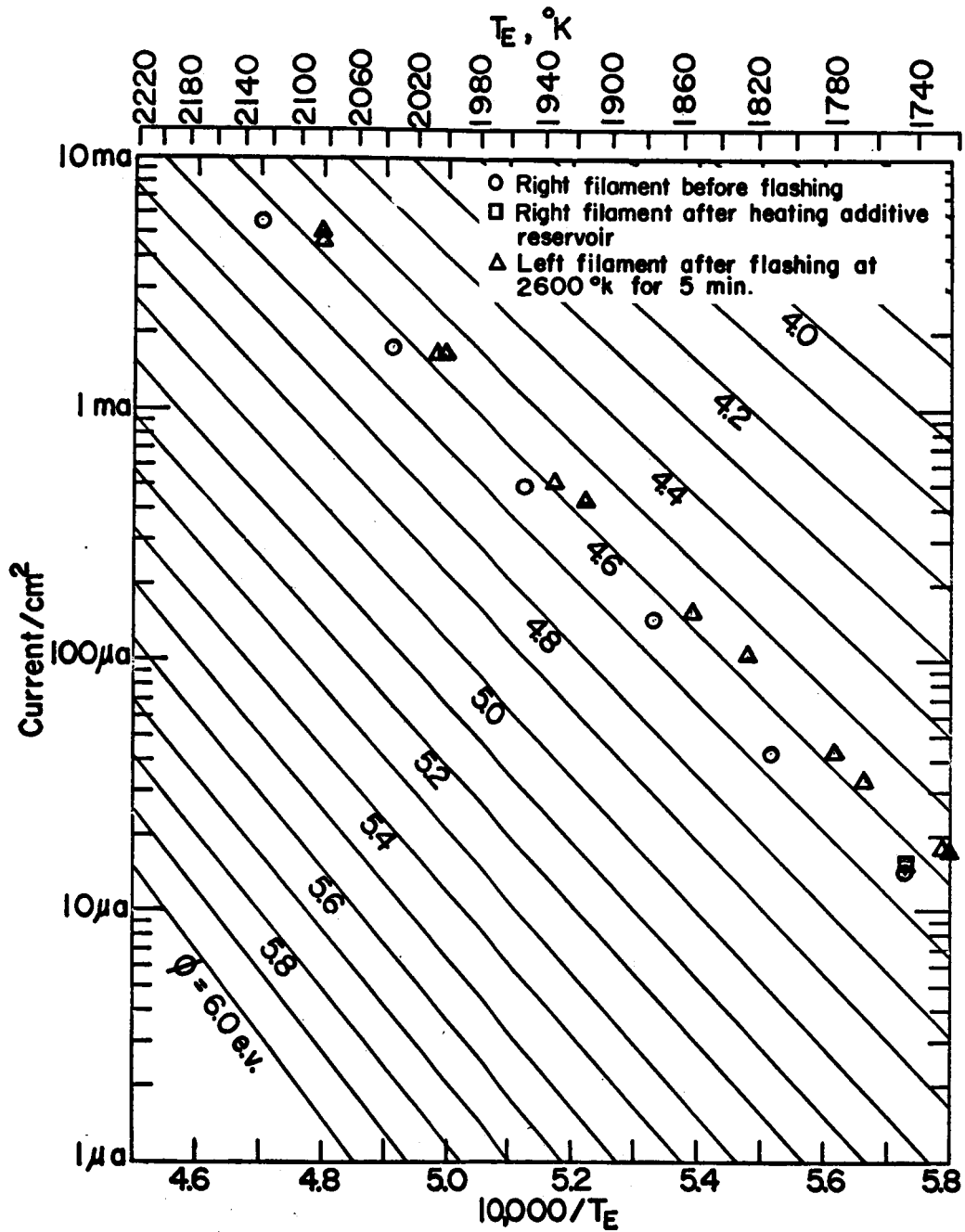
Figure II-17. Right Filament φ with Liquid Nitrogen Cooling

Before each day's run, the filaments in the test vehicle were held at about 1900 °K for one-half to one hour. The resultant heating of the test vehicle removed adsorbed gases on the walls and on the filaments. A burst of gas to about 10^{-7} torr was observed initially followed by a recovery to 10^{-9} torr. The pressure then rose slowly to 10^{-8} as the walls became heated and recovered to 10^{-9} near the end of the heating time. After cooling to liquid nitrogen temperature, a final pressure of 10^{-11} torr was obtained. A final flash to 2600 °K for three minutes stripped the filament of any adsorbed layers prior to testing. Throughout the testing the maximum pressure observed was 5×10^{-10} torr and was below 5×10^{-11} most of the time.

In steady state experiments, the reservoir was heated to the desired temperature and the J-V characteristics at each of several filament temperatures were determined. The presence and arrival rate of CsF was evaluated from the current in the ion accelerating portion of the characteristic. Figure II-18 shows typical curves for two different filament temperatures. The ion current change is due to a drift in reservoir temperature and not to the filament temperature change.

Transient behavior was examined by applying a step function current change to the unheated filament and plotting the emission current as a function time. Plots were made both with and without CsF and samples are shown in Figures II-19 and II-20. A variable delay, dependent on the time since the filament was last heated, appeared in the bare runs. By following a specific cold, preheat, and final current time schedule for each run the variations were held to about 0.1 sec.
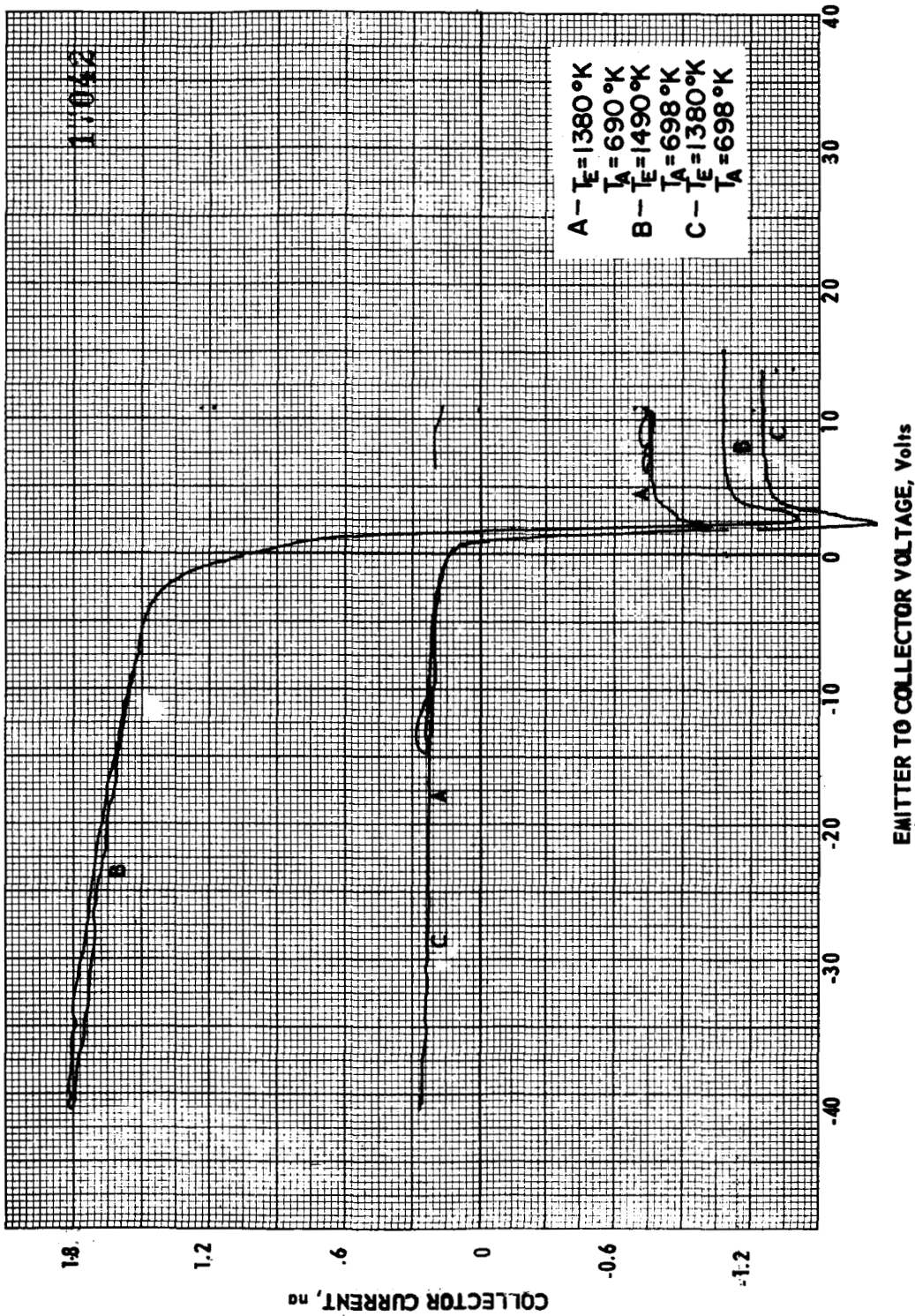
Figure II-18. Typical J-V Characteristic Showing Ion Currents
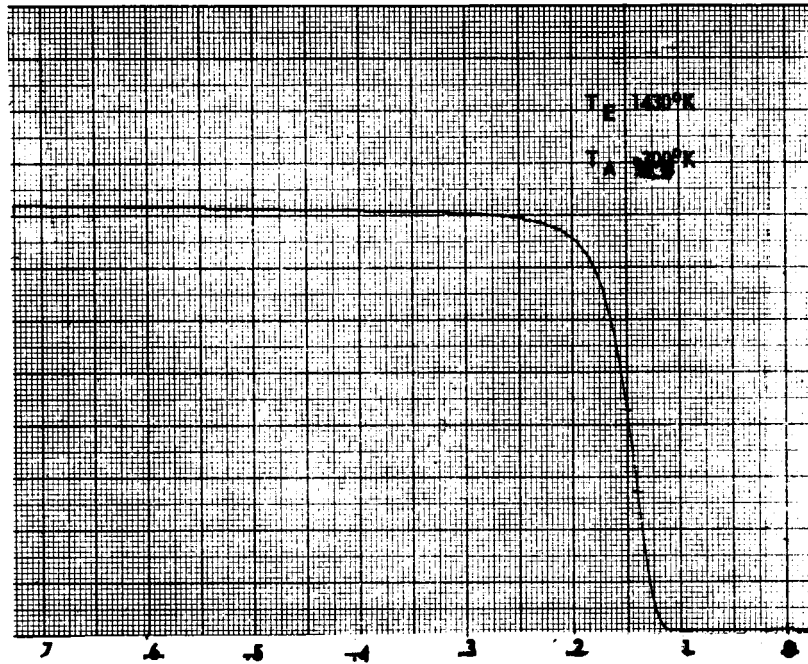
Figure II-19. Emission Current Transient with No CsF
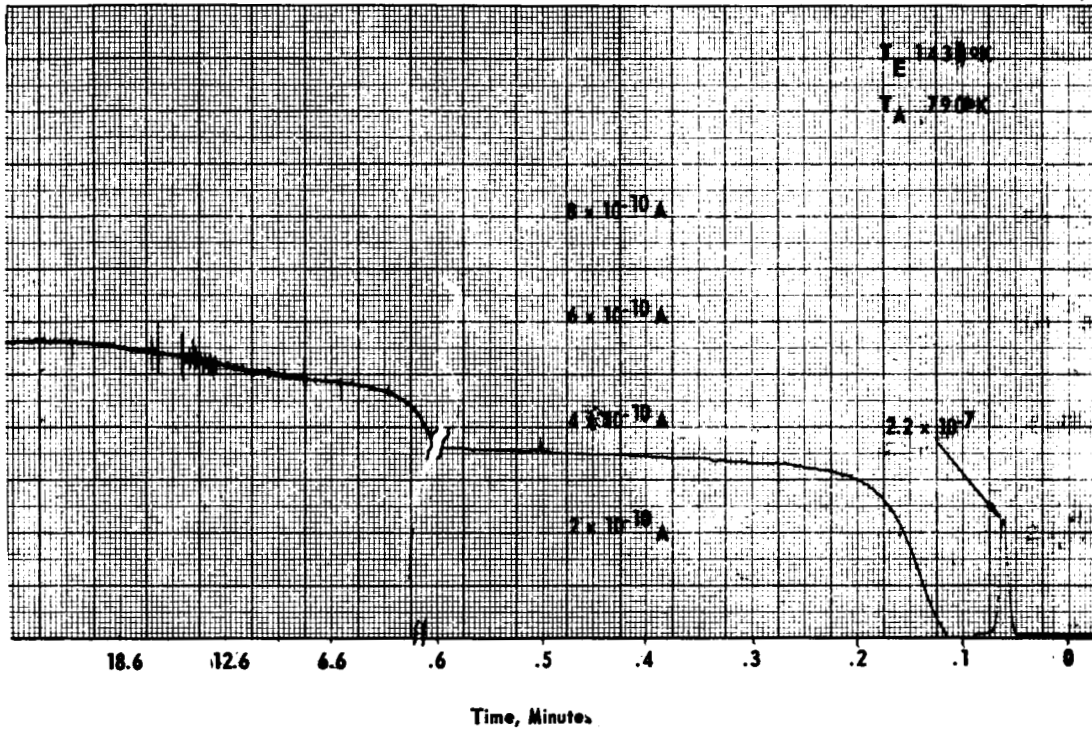
Figure II-20. Emission Current Transient with CsF

5. Results

Using the saturation current values from the J-V characteristic, work functions for each filament temperature were calculated and are plotted in Figure II-21. This figure shows points for arrival rates from 0.2 na/cm^2 to 1.2 na/cm^2 as well as data for the bare filament. The work function change was on the order of 0.07 to 0.1 eV and was apparent only at very low emitter temperatures (1300-1500 °K). The corresponding particle arrival rate for the CsF is from 3×10^9 to 2×10^{10} particles/cm^2 - sec which is still rather low. This is probably the reason the effects are evident only at low filament temperatures, although the absence of any pronounced changes in the transient characteristics indicates that the adsorption energy is rather small.

An interesting feature of the transient characteristic is the very large current peak appearing shortly after the start of the current step. Dissociation of the CsF is believed to cause a build up of a Cs adsorbed layer which lowers the work function at low temperatures. As the filament heats, therefore, it passes through the maximum current on the Taylor Langmuir S curves. At higher temperatures, the Cs cannot remain on the filament and its effects disappear. This peak is further evidence that there is actually CsF present in the device.
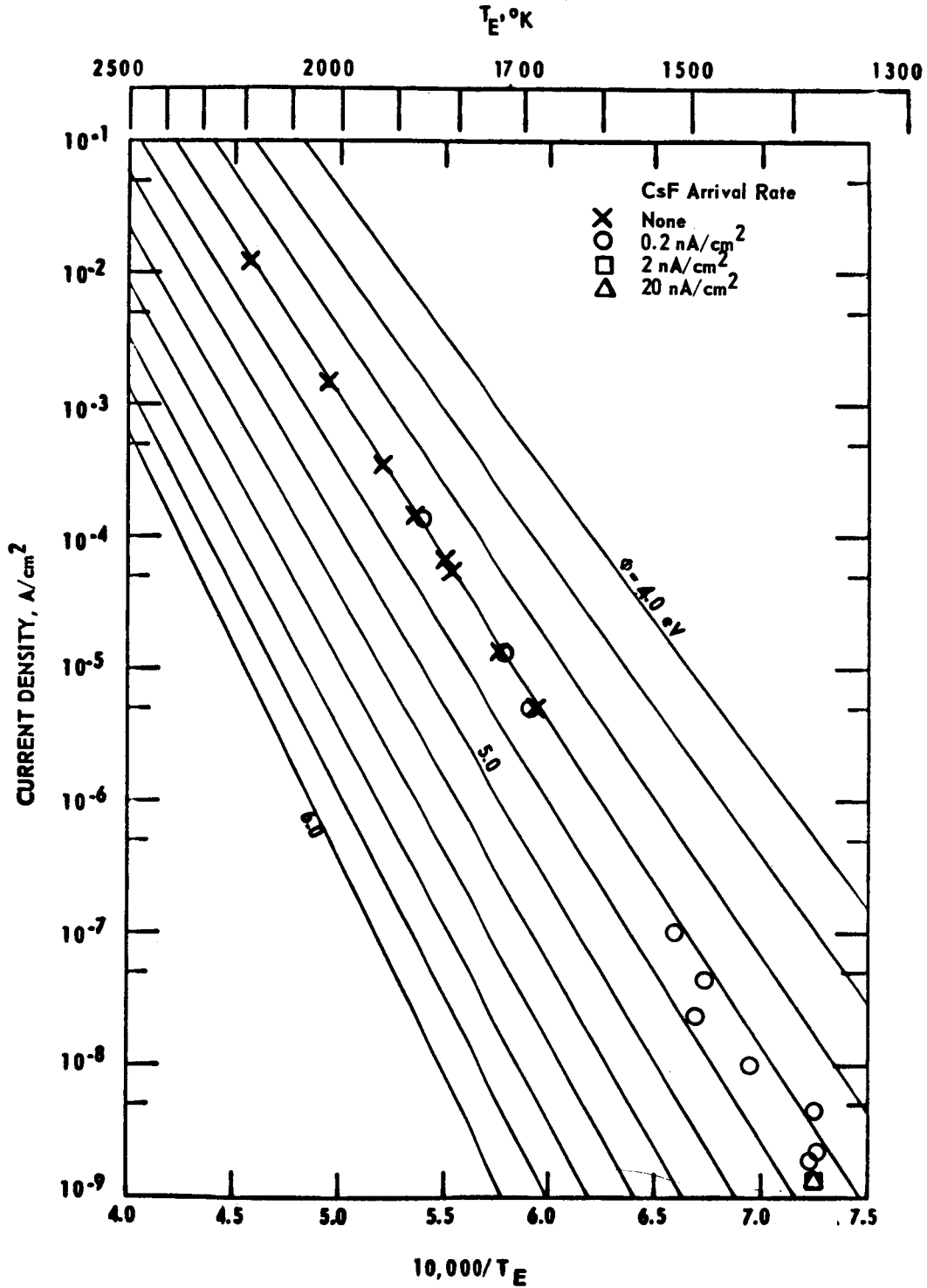
Figure II-21. Work Function Results with CsF

CHAPTER III

O$_2$ SURFACE ADDITIVE

A. GENERAL

The preceding chapter presented experimental evidence to the effect that the short-lived high converter performance previously attributed to cesium fluoride was in fact, due to oxygen contained in the form of water in the CsF crystals. Pure CsF has been shown to be much less effective than O$_2$ in altering the work function of tungsten and at this time holds little promise as a surface additive, although continuing investigations may yet show that fluorine can be useful under conditions which have not yet been explored. These considerations prompted a re-evaluation of oxygen as an electronegative surface additive with the objective of exploiting its desirable characteristics for indefinite periods of time, avoiding of course any deleterious effects.

B. OXYGEN ADSORPTION CONSTANTS

The ability of adsorbed oxygen films to raise the work-function of tungsten and also render cesium more effective in subsequently lowering it, was first reported by Kingdon[1] in 1924. Since then several communications have appeared in the literature regarding experiments in which the work-function change and adsorption constants for oxygen on tungsten were measured. By 1935, two new methods of experimental study of oxygen films had been reported. Roberts[5] used the accommodation coefficient of neon on tungsten filaments to detect the presence of oxygen and Johnson and Vick[6] used an oscillograph to measure the time constants of O$_2$ desorption. Langmuir and Villars[4] also published, in 1931, their results with O$_2$ and Cs which they regarded as a method of detecting oxygen at extremely low partial pressures. The phenomenon was the

III-1

subject of considerable controversy at the time as is evident in A. L. Reimann's[7] communication presenting his own work and attacking Kingdon's inclusion of the temperature dependence of work function in the pre-exponential constant. Progressively more sophisticated studies of the adsorption and diffusion of oxygen on tungsten were performed using the accommodation coefficient technique, developed by Roberts, and field emission, first applied by Müller[8]. Both approaches have been very effective in defining the physics of the system in the temperature range of 4.2 to 700°K. The first significant experimental advance at thermionic emitter temperatures (above 500°K) since the work of Langmuir, Johnson and Vick, and Reimann, however, is that reported by Engelmaier and Stickney[9]. These investigators have measured adsorption energy values and work-function changes under various conditions of coverage. A summary of their data is shown in Table I. Inspection of Table I shows that the maximum reported work function change caused by adsorbed oxygen varies between 0.7 and 0.95 eV. Larger differences, as much as 1.8 eV, have been reported by Reimann[7] and Gomer and Hulm[10]. Reimann used contact potential measurements while Gomer used field emission; in both cases, the emitter temperatures were very low, less than 700°K. It is doubtful that these low temperature measurements are applicable to emission at thermionic temperatures because there is no reason to believe that the character of the adsorbed oxygen film is not greatly altered when the temperature is increased.

The desorption energy values listed in Table I vary from 140 to 160 k cal/gram-atom of O_2 and are in fact in good agreement with one another. The most extensive and well-controlled study is that of Engelmaier who measured both work function and desorption energy as a function of oxygen pressure and surface temperature. For the remainder of this discussion the 140 k cal/gram-atom value of desorption energy shall be used.

TABLE III-1

Reference	$\Delta\phi_{max}$	E_o	Type of Measurement
Langmuir, Kingdon Phys. Rev. 34 129 -(1929)	0.8 eV (at T > 1500 °K)	—	Emission and Contact Potential
Langmuir Ind. & Eng. Chem. 22, 4 p. 390 (1930)		$160 \frac{k\ cal}{gr\ atom}$	Emission transient
M. C. Johnson F. A. Vick J. Am. Ch. S. 53, 486 (1931)	—	$147 \frac{k\ cal}{gr\ atom}$	Emission transient
J. K. Roberts Proc. Roy Soc. A154, 464 (1935)	—	$140 \frac{k\ cal}{gr\ atom}$	Accommodation coefficient of Neon
A. L. Reimann Phil. Mag. 20 594 (1935)	0.7 eV (at T > 1500)	—	Contact Potential
Engelmaier & Stickney Phys. El. Conf. Proceedings 1966 Mass. Inst. Tech.	0.95 eV (at T > 1500)	$140 \frac{k\ cal}{gr\ atom}$	Emission

The time rate of desorption of oxygen particles from the tungsten surface is given by

$$\frac{d\sigma}{dt} = A\sigma e^{-E/kT} \qquad * \qquad (1)$$

where σ is the density of adsorbed particles, A is a frequency factor approximately equal to kT/h, E is the energy for desorption, T is temperature of the surface, k the Boltzmann constant and h is the Planck constant. Under steady state conditions, the rate of departure of oxygen particles must equal the arrival rate, J_μ:

$$J_\mu = \frac{kT}{h} \sigma e^{-E/kT} \qquad (2)$$

Equation (2) was used to compute the pressure of oxygen required to maintain full coverage as a function of temperature, assuming that $\sigma = 4.6 \times 10^{14}$ cm^{-1} and E = 140 k cal/g-atom. The results are plotted in Figure III-1. Note that the oxygen pressure necessary to maintain a significant change in work function is less than 10^{-6} torr for emitter temperatures up to 2000°K. This result is in good agreement with the observations of Engelmaier.

C. CHEMICAL EQUILIBRIUM

In the preceding section experimental and theoretical evidence was used to estimate an upper limit for the oxygen pressure required to achieve an "additive effect" on a tungsten emitter. It is the objective of this section to examine whether this oxygen pressure can be compatible with the materials and operating conditions of the converter.

---

* This relation does not necessarily yield an exact measure of the desorption process but it does furnish an order of magnitude estimate which is in fact the objective of this computation.

THERMO ELECTRON
ENGINEERING CORPORATION
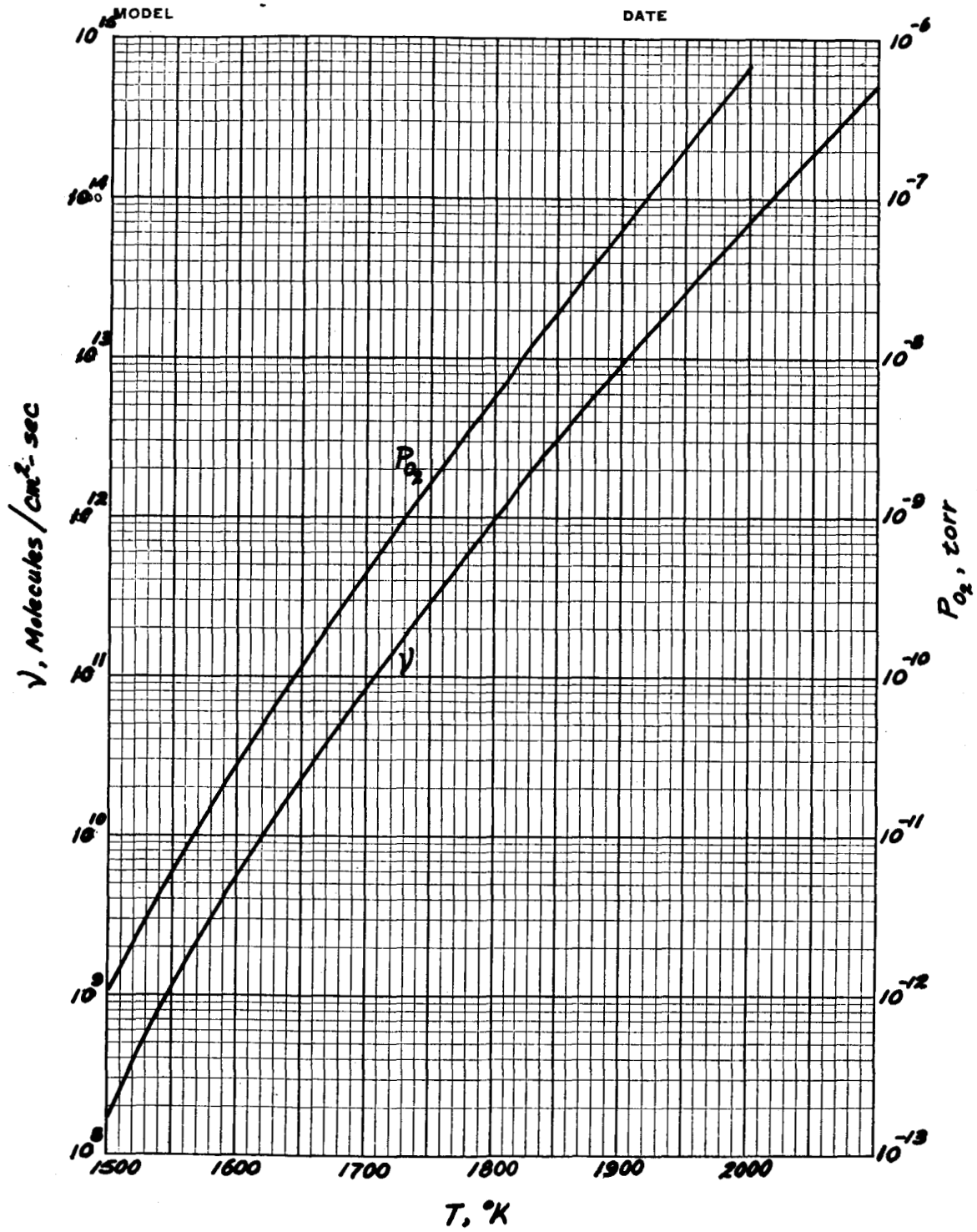
Figure III-1. Required Oxygen Pressure as a Function of T_E.

In general, metals react with oxygen to form oxides in accordance with the following reaction:

$$x\,O_2 + yM \rightarrow M_yO_{2x} \;. \tag{3}$$

A free energy change is associated with the reaction usually referred to as the free energy of formation of the metal oxide. The free energy of formation, ΔF, is a function of temperature and is related to the equilibrium constant, K, of the reaction by:

$$-\Delta F = RT \ln K, \tag{4}$$

where R is the gas constant and T is the temperature of the system. Assuming that the oxygen pressure is low enough so that the perfect gas laws apply and that the metal and its oxide are solids, the equilibrium constant can be expressed in terms of the oxygen pressure and the activities, α, of the solid phases.

$$K = \frac{\alpha_{M_yO_{2x}}}{\alpha_M^y \cdot P_{O_2}^x} \tag{5}$$

Since the activity coefficients are equal to unity for the system considered here, we may write

$$K = \frac{1}{P_{O_2}^x} \;. \tag{6}$$

In the case of the cesium-oxygen equilibrium where the metal exists in the gaseous state,

$$K = \frac{1}{P_{Cs}^4 \, P_{O_2}} \;. \tag{7}$$

Figure III-2.   Equilibrium O_2 Pressure Over Various Metal
Oxides.

It follows then, that the equilibrium pressure of oxygen above a metal oxide is fixed, at any given temperature. If the oxygen pressure is increased above this equilibrium value, the chemical reaction (3) will proceed to the right, i.e., more oxide will b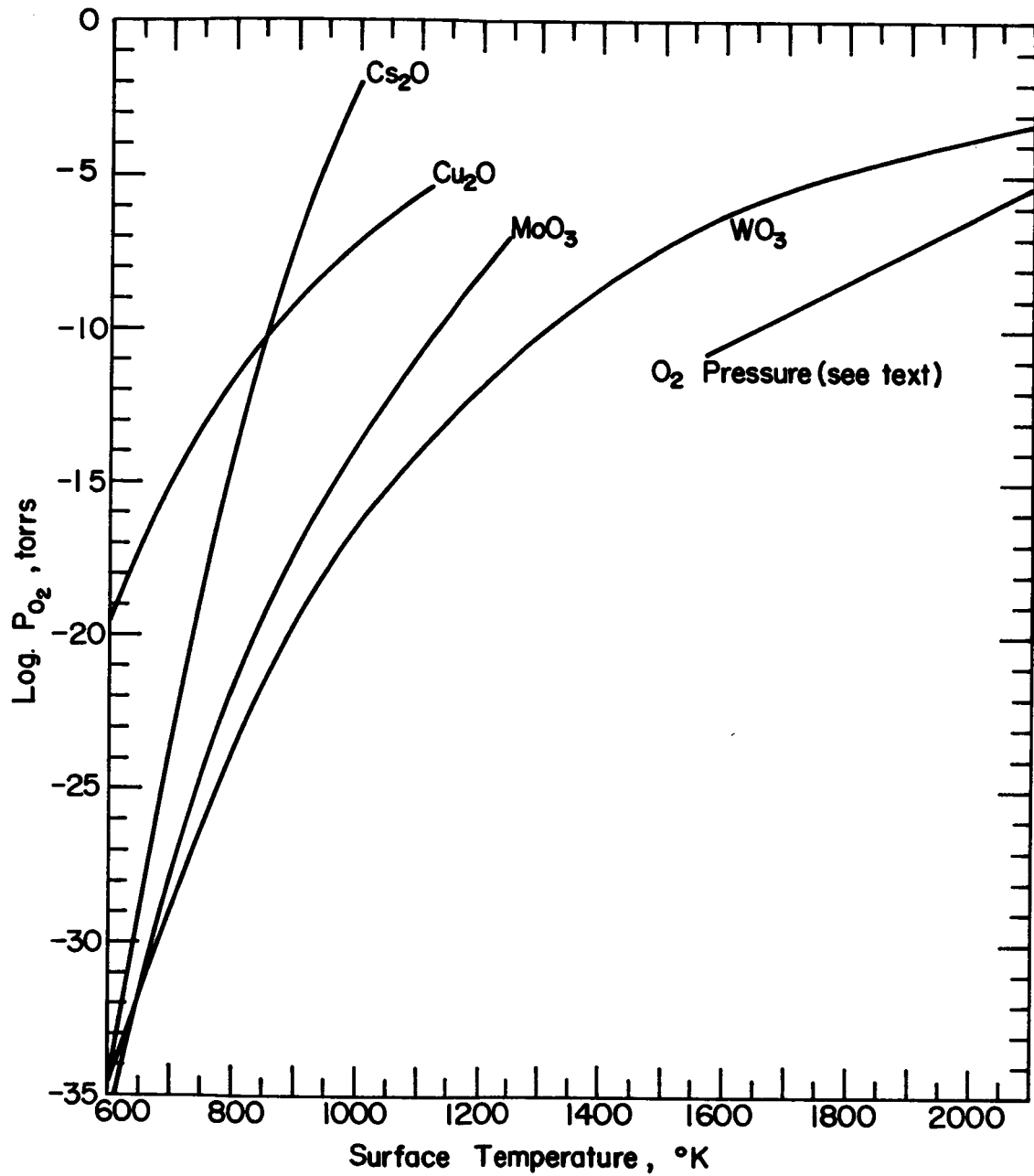e formed until one of two things happen. Either the oxygen pressure is reduced to the equilibrium value, or all the free metal is consumed in the formation of oxide. If the oxygen pressure is maintained below the equilibrium value all the oxide will decompose. It is possible, then, to maintain a metal in an oxygen atmosphere at any temperature without any oxidation taking place provided the oxygen pressure is less than the equilibrium pressure above the oxide.

The equilibrium pressure of oxygen above Cs_2O, Cu_2O, MoO_3 and WO_3 was computed as a function temperature using the relations outlined above and free energy of formation data from Reference 11. The results are plotted in Figure III-2 in terms of $\log P$, torr, versus temperature. A line labeled " oxygen pressure" is also shown in this figure. This line is a plot of the oxygen pressure required for substantial coverage on the emitter surface, shown in Figure III-1. For example, for an emitter temperature of 1900 °K the oxygen pressure required is 5×10^{-8} torr which is well below pressure of O_2 in equilibrium with WO_3 so no tungsten oxide will form. MoO_3 will not form at temperatures higher than 1200 °K, Cu_2O at temperatures higher than 980 °K and Cs_2O at temperatures higher than 900 °K. The 1200 °K limit is higher than the ordinary operating temperatures molybdenum collectors. It is, however, close enough to normal collector operating temperature so that it is not at all clear that it can be considered a limiting factor on the basis of this rough calculation.

The cesium reservoir and other cold areas of the converter will certainly constitute sinks for oxygen. To use, therefore, oxygen as an additive, it is necessary to introduce it directly into the interelectrode space and to provide a continuous flow of it, since it will constantly be lost through the gap at the emitter and collector edges. The amount of oxygen lost in this manner can be estimated by,

$$G = 5.83 \times 10^{-2} \, P \sqrt{\frac{M}{T}} \, A \, t, \tag{C}$$

where G is the total mass in grams that flows through area A at pressure P and temperature T in time t; M is the molecular weight of oxygen. Assuming:

$$P = 10^{-6} \text{ torr}$$
$$A = 7.83 \times 10^{-2} \text{ cm}^2 \text{ (2 cm diameter emitter - 0.005" gap)}$$
$$T = 1000 \, ^\circ K$$
$$t = 3.6 \times 10^7 \text{ sec (10,000 hours)}$$

We find that 32 mg of oxygen will be consumed, a very small quantity indeed.

D. CRITICAL EXPERIMENT

On the basis of the above discussion, an experiment was devised to determine whether this reasoning was indeed correct. For the results of such an experiment to be conclusive, a true steady state condition had to be established, i.e., the addition of oxygen could not be a batch addition, the effect of which would then decay over a period of time.[*] To provide the necessary oxygen

---

[*] All previous work cited above as well as power production experiments by Wilson[12] and Levine[13] used a time transient approach, albeit the time constant was long in some experiments.

in the range of 10^{-8} to 10^{-6} torr continuously and in a controllable fashion, it was decided to use an oxygen compound which would release oxygen at the proper pressure by reversible decomposition when heated to the appropriate temperature. Cesium oxide was selected because it satisfies these requirements, but in addition, it permitted the use of an existing converter by oxidizing part of its cesium. A converter equipped with a connection to a gas injection system was selected. The cesium was first condensed in the vicinity of the collector and, with the converter at room temperature, 50 mg of oxygen were introduced and consumed immediately in oxidizing the cesium. The Cs_2O formed, served as the source of O_2. Emitter work function measurements were made with Cs and Cs_2O and the values obtained duplicated previous "CsF" results, (see Figure III-3). Performance data were generated subsequently and a summary of these results is shown in Figure III-4. The two envelopes in this figure, for Cs and Cs and Cs_2O, show the typical two-fold increase in power output caused by the additive. Once the performance superiority of the converter was established, the device was placed on a short life test for 130 hours as a check of stability. No changes in the output of the converter were observed except for apparently random fluctuations of $\pm 5\%$. After one week of life test, the converter was dismantled and examined for evidence of chemical action on the electrode surfaces; none was found.

Almost all the hypotheses regarding the use of oxygen advanced above were confirmed by these results giving strong indications that oxygen could be used as a surface additive on a steady state basis.
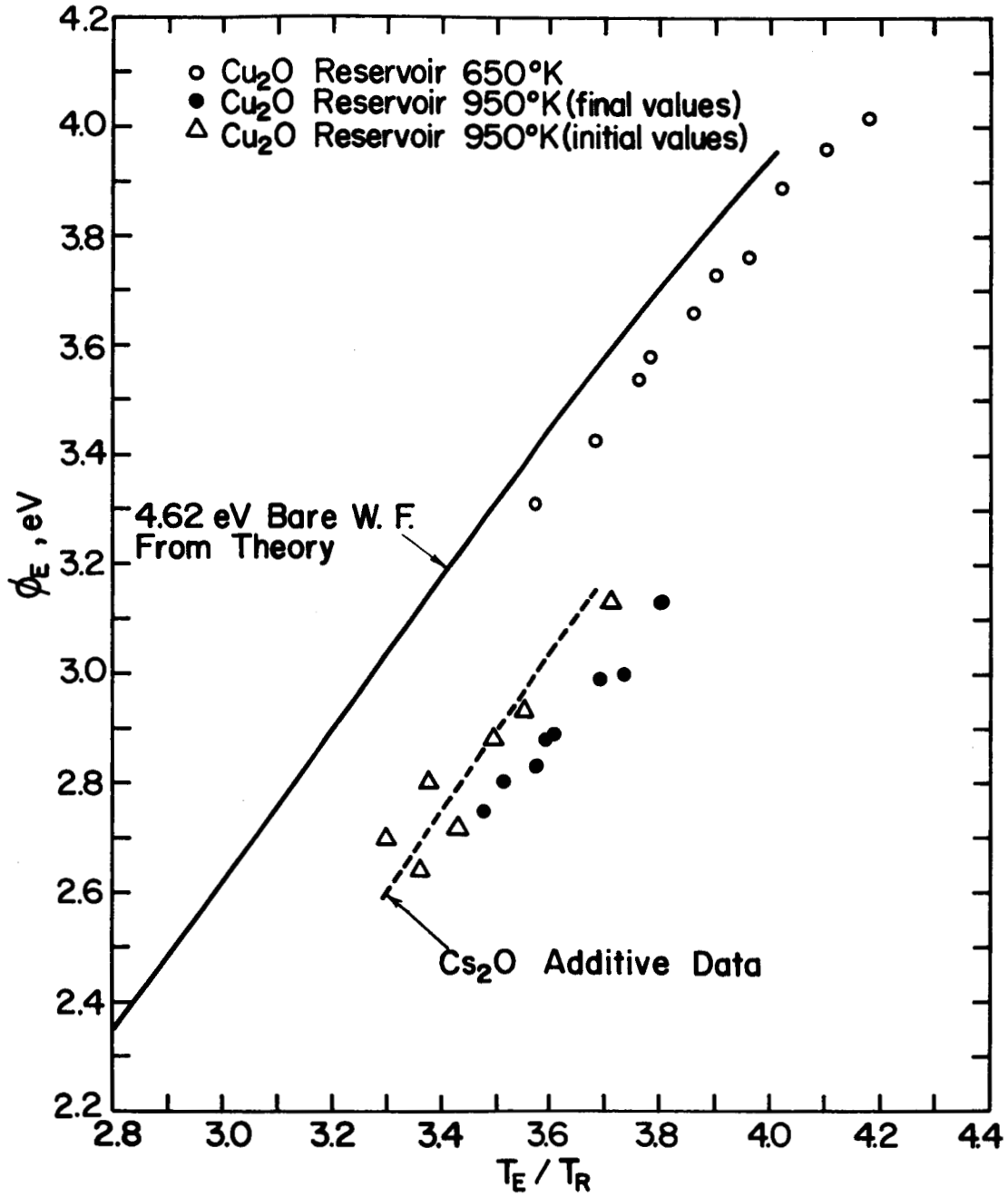
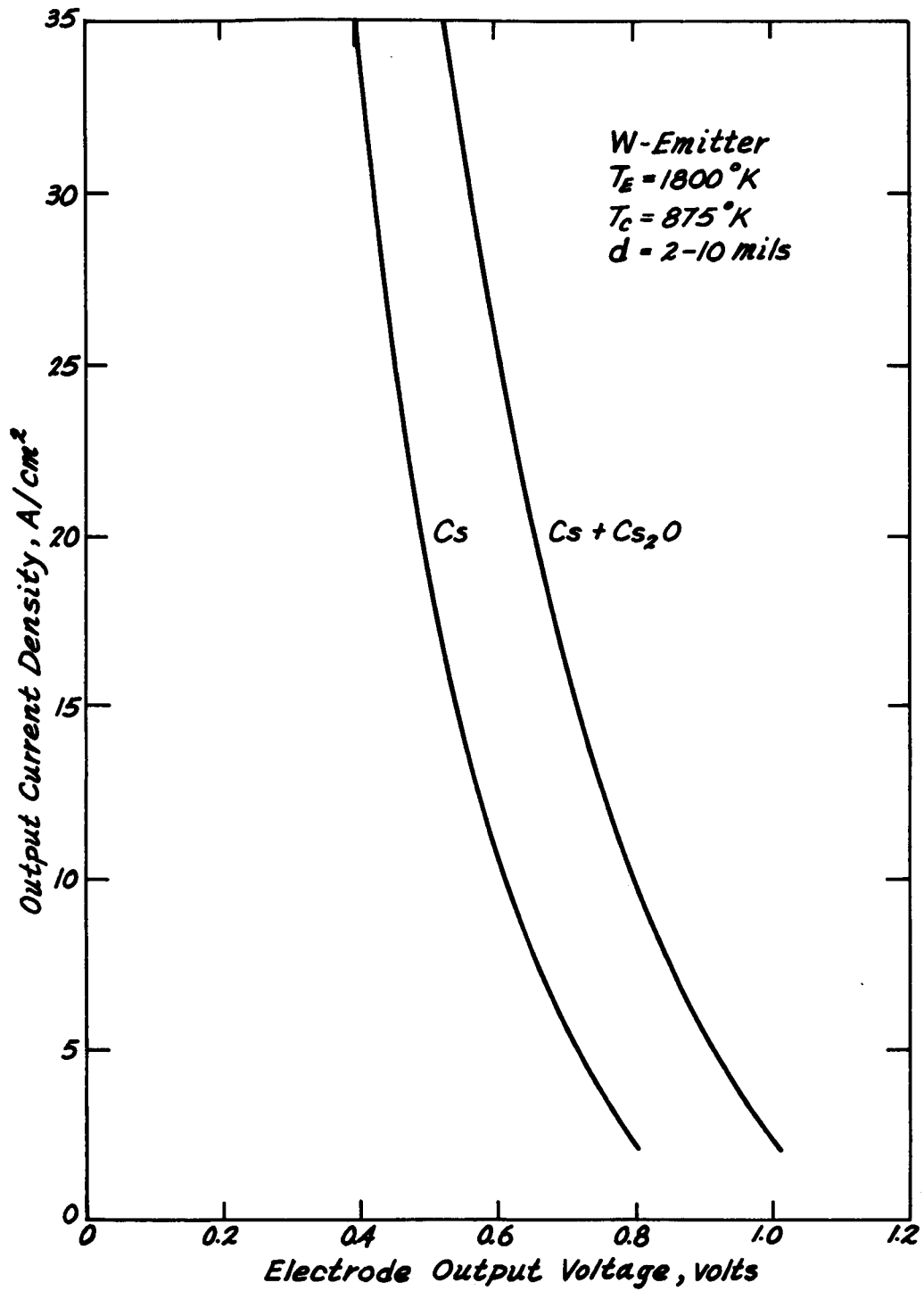Figure III-3. Additive ϕ vs T/T_R.

Figure III-4. Performance Envelope With Cs_2O and Cesium.

E. EXPERIMENTAL RESULTS

The success of the critical experiment lead to the construction of a special converter equipped with an additive reservoir located below the collector. A tube through the center of the collector connected the additive reservoir to the interelectrode gap. This arrangement allows oxygen from this reservoir to flow to the interelectrode space without coming in contact with any cold surfaces.

Oxygen was supplied by the decomposition of Cs_2O in the critical experiment. In that instance, this approach proved satisfactory, but it does suffer from the limitation that the vapor pressure of O_2 in equilibrium with Cs_2O is a very strong function of temperature. Inspection of Figure III-2 will show that the pressure curve for Cs_2O is the steepest in the group. Cu_2O, on the other hand, shows a much less steep slope; O_2 pressure increases an order of magnitude every 60°K. Cu_2O, is therefore, a much more suitable compound for our purpose. It does not evaporate as a molecule, but decomposes instead which is, of course, a basic requirement of any O_2 source.

The new converter was charged with a Cu_2O pellet and cesium. Testing was started with a series of emitter work function determinations. Emitter work function values were determined by measuring the emitter saturation current under ion rich conditions ($\phi_E > 2.7$ eV) using small interelectrode spacings (d < 1 mil) to avoid electron space charge and scattering. A series of runs was made with the additive reservoir at 675°K corresponding to an oxygen pressure below 10^{-14} torr. The work function values obtained, shown in Figure III-3 as open circles, are typical of treated polycrystalline tungsten. The solid line shown corresponds to a bare work function value of 4.62 as computed from Rasor's[14] theory and has been included for reference purposes.

III-13

The next series of runs were taken after heating the additive reservoir to 950 °K resulting in an oxygen pressure of 10^{-8} torr. The first work function measurements made, a few hours after the additive temperature was raised, are shown as triangles in Figure III-5. As time went on, the work function continued to decrease for a given value of T/T_R for approximately 20 hours. At the end of this period of time, it stabilized along a line defined by the solid circle points. This terminal value is somewhat lower than the data obtained with CsF reported in Ref. 15, and shown as a dashed line in Figure III-3. Comparison of the cesium only data (open circles) with the equilibrium additive data (full circles) shows that the addition of oxygen has resulted in a reduction of approximately 0.45 eV in the emitter work function, for the same T/T_R ratio.

The effect of the additive on collector work function was also investigated. Retarding plots were used to measure collector work function in accordance with the procedure described in Ref. 15. The results of these measurements are shown in Figure III-5 which is a plot of collector work function versus the ratio of the collector to cesium reservoir temperature. Also shown in this figure is the work function of a moly collector without additive from Ref. 15. The effect of the additive has been to shift the minimum collector work function value from a temperature ratio of 1.8 to 1.45 while the minimum value itself has remained 1.45 eV.

At the time of completion of the electrode work function measurements, 55 hours of testing had passed since the additive reservoir was first heated to 950 °K and 35 hours since a stable, equilibrium, work function value was obtained.
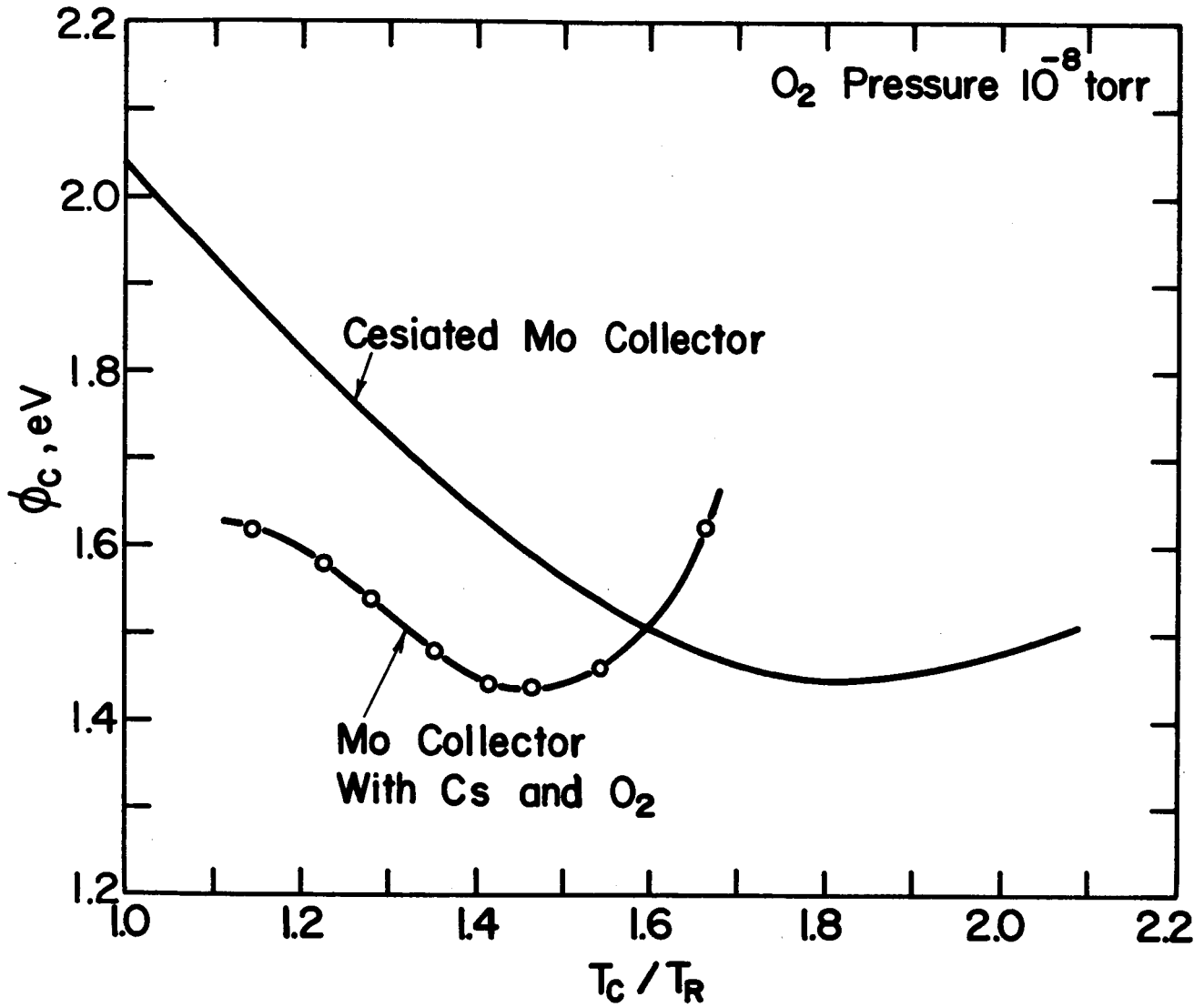
Figure III-5. Cesiated Collector Work Function Comparison.

The next series of experiments consisted of performance parametric data mapping. Figures III-6 and III-7 show data obtained at 1760 °K emitter temperature with 5 and 10 mil spacing respectively. Similar data from a polycrystalline tungsten emitter[16] is shown in Figures III-8 and III-9. Two significant features of the oxygen converter characteristics when compared to the Cs only data are the greatly decreased Cs temperatures for a given saturation current, as much as 60 °C in some cases, and the steeper slope of the envelopes in the oxygen device. The slope change is a direct result of the lowered Cs pressure through the reduction in scattering. This data is being used in the preliminary evaluation of the device. A wide range of collector temperatures and spacings will be investigated to form a complete performance map.

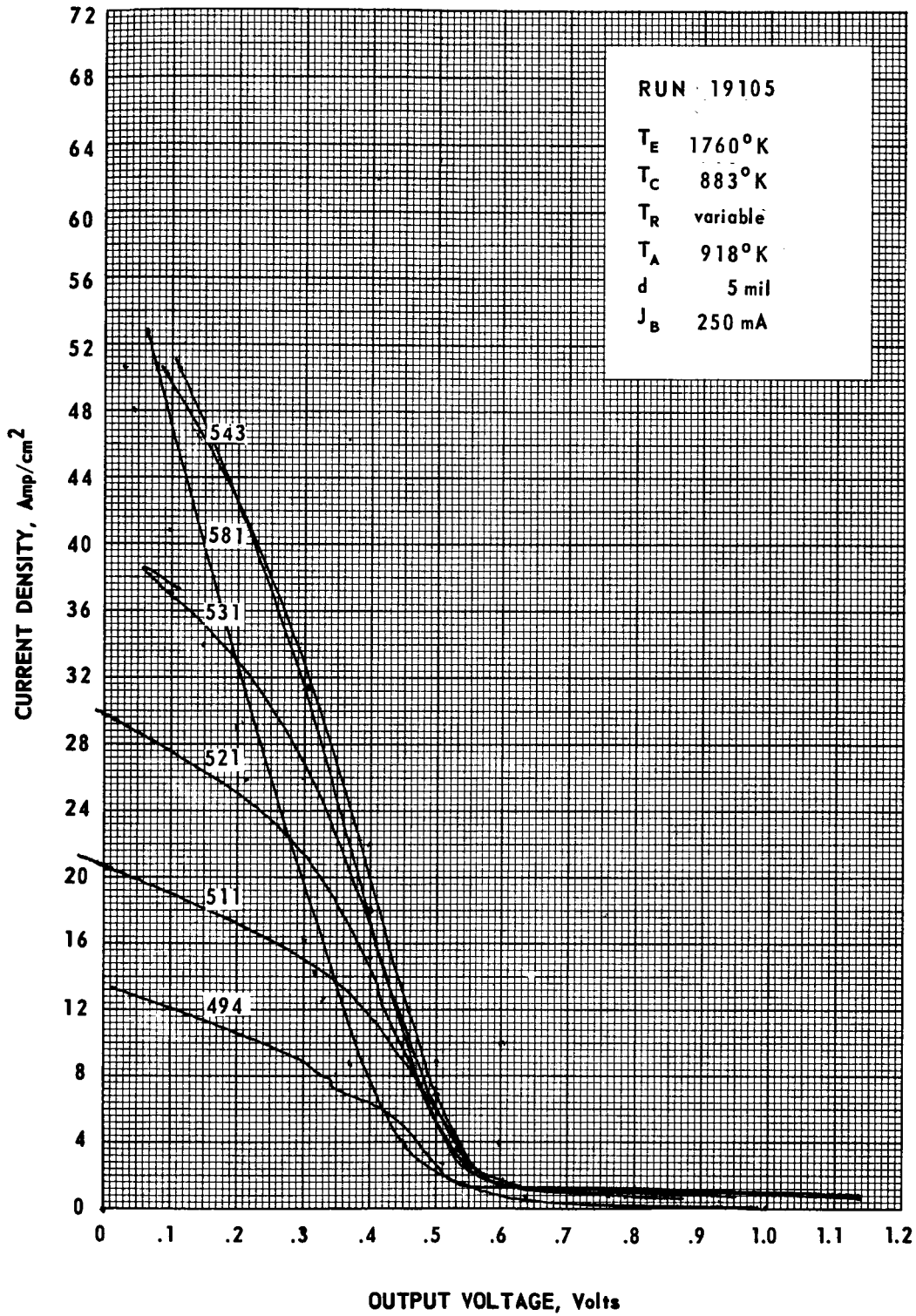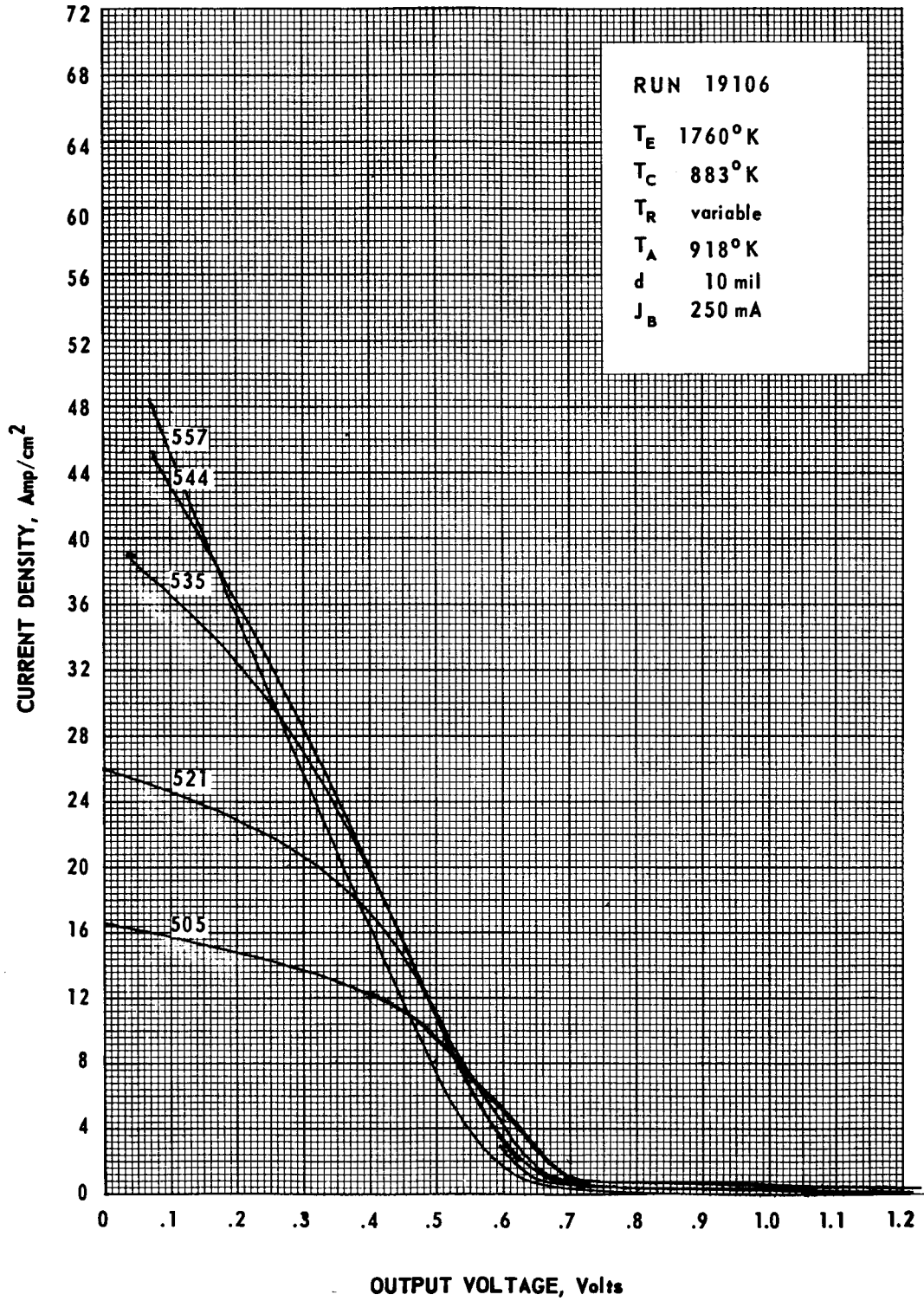Figure III-6. J-V Family With Cesium-Cu$_2$O Converter.
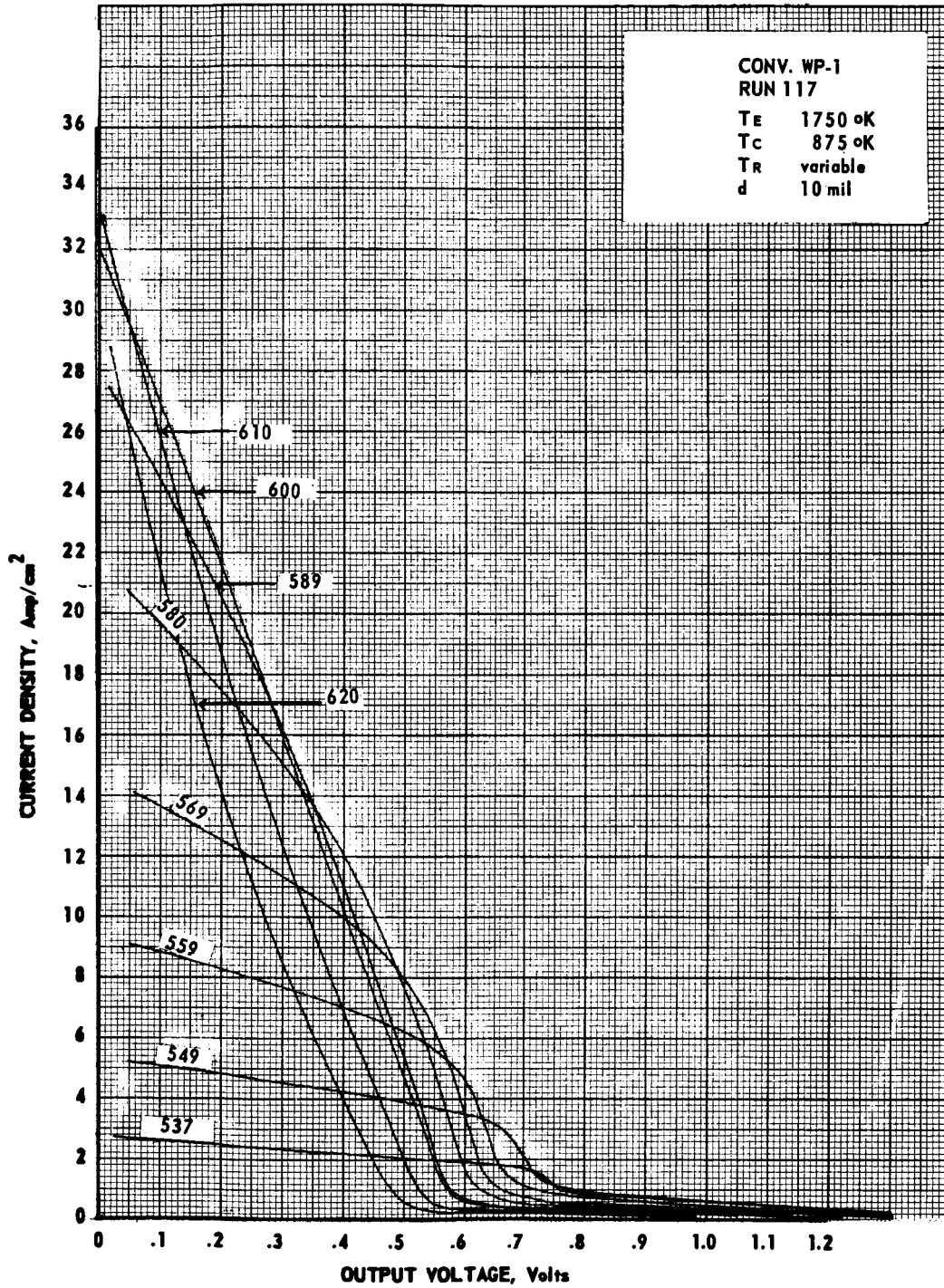
Figure III-7. J-V Family With Cesium-Cu$_2$O Converter.

Figure III-8. J-V Family With Cesium Only Converter.
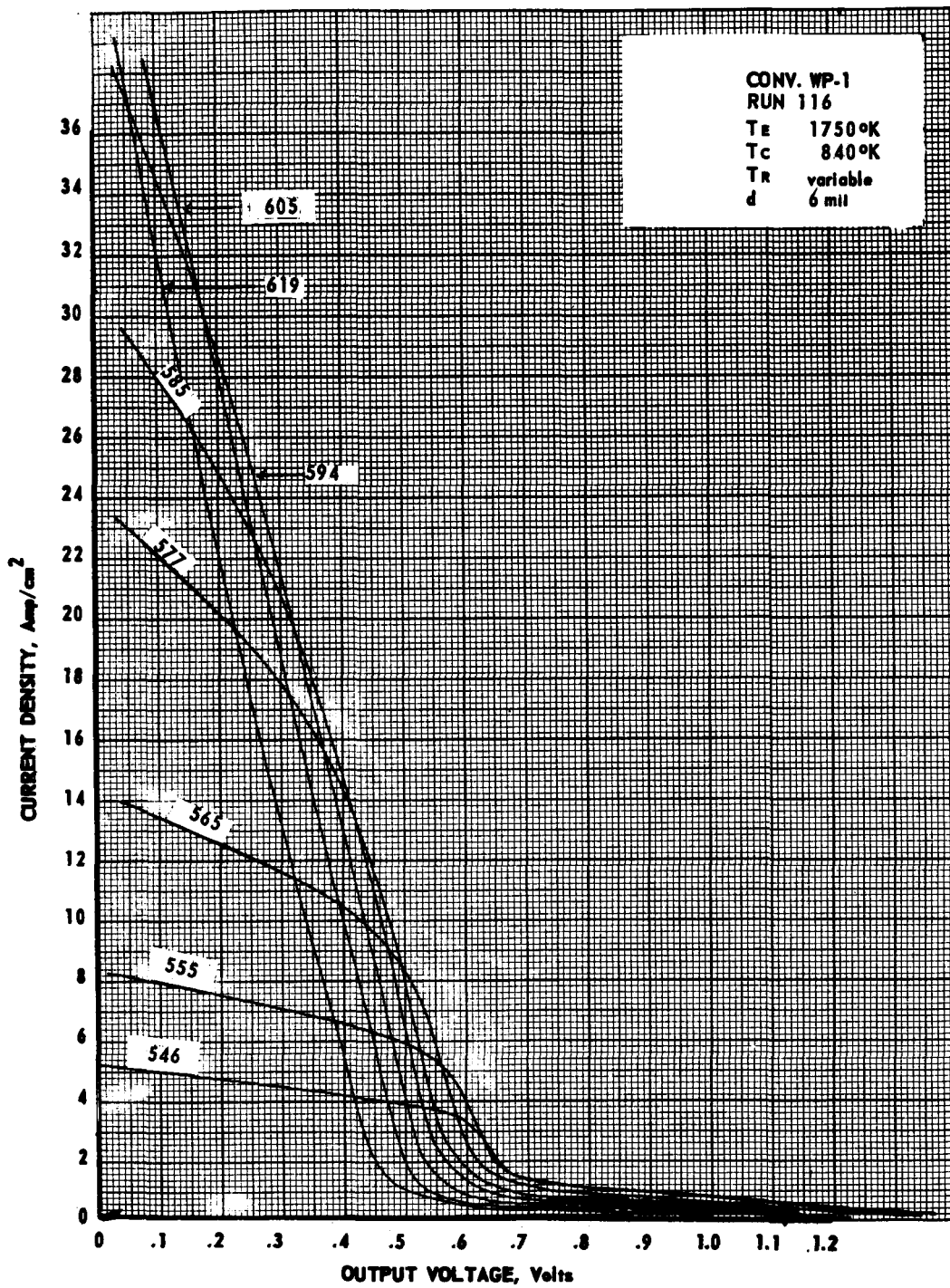
Figure III-9. J-V Family With Cesium Only Converter.

REFERENCES

1. K. H. Kingdon, Phys. Rev. <u>24</u>, 510 (1924)

2. I. Langmuir and K. H. Kingdon, Phys. Rev. <u>34</u>, 129 (1929)

3. I. Langmuir, Ind. and Eng. Chem. <u>22</u>, 390 (1930)

4. I. Langmuir and D. S. Villars, J. Am. Chem. Soc. <u>53</u>, 486 (1931)

5. J. K. Roberts, Proc. Roy. Soc. <u>A152</u> 464 (1935)

6. M. C. Johnson and F. A. Vick, Proc. Roy. Soc. <u>A151</u> 308 (1935)

7. A. L. Reimann, Phil. Mag. <u>20</u>, 594 (1935)

8. E. W. Müller, Ergelo. exakt. Naturw. <u>27</u>, 290 (1953)

9. W. Engelmaier and R. Stickney, Proc. Phys. El. Conf. M.I.T., (1966)

10. R. Gomer and J. K. Hulm, J. Chem. Phys. <u>27</u>, 1363 (1957)

11. C. E. Wicks and F. E. Block, Bulletin 605, Bureau of Mines, U.S. Dept. of Interior. (1963)

12. V. C. Wilson, Proc, Therm, Conv. Spec. Conf., IEEE, Gatlinburg, Tenn. p. 121 (Oct. 1963)

13. J. D. Levine, Proc, Therm. Conv. Spec. Conf., IEEE, San Diego, Calif., p. 276, (Oct. 1965)

14. N. S. Rasor and C. Warner, J.A.P. <u>35</u>, 2589 (1964)

15. Kitrilakis, et al, 4040 Final Report NASA-JPL Contract No. 950671, Thermo Electron Eng. No. TE 7-66, (Aug. 1965)

16. Miskolczy et al, Final Report NASA-JPL Contract No. 950228, Thermo Electron Eng. No. TE 63-64 (Feb. 1964)

CHAPTER IV

INERT GAS EXPERIMENTS

A. GENERAL

The study of the interactions of inert gases with the ignited mode cesium plasma of the converter was undertaken for two reasons. (a) The inert gases provide an additional tool with which the ignited mode plasma can be investigated and various transport parameters evaluated. (b) There is a strong possibility of improving converter performance by exploiting the fact that inert gas atoms retard the loss of Cs ions to the electrodes while they are essentially transparent to electrons. Both objectives require and understanding of electron scattering by inert gas atoms. A theoretical analysis of this process was presented in the Second Quarterly Report[IV-1]. A brief summary of that analysis is given here followed by comparison with experimental results obtained during the current reporting period.

The last section of this chapter presents a summary of parametric data obtained with Cs only and designed to serve as a reference to which similar data in the presence of argon can be compared.

B. ANALYSIS

The diffusion equation was solved for the plasma region bounded by the emitter and collector sheaths with the assumptions that the interelectrode spacing is larger than the electron mean free path and that the velocity distribution of the electrons is Maxwellian. The solution is

$$\frac{1}{J} = \frac{1}{J_s} + K \exp \left[\frac{eV}{kT_{\epsilon\epsilon}} \right] \left[\frac{3}{4} (\Sigma_1 + \Sigma_2) d + L \right], \tag{1}$$

where

$$K = \frac{1}{J_s} \exp \left[- \frac{\phi_E - \phi_C + V_C}{kT_{\epsilon E}} \right] \tag{2}$$

and

$$L = \exp \left[V_C / kT_{\epsilon} \right] - 1 \tag{3}$$

J and J_s are the net and saturation electron currents respectively, V is the output voltage, $T_{\epsilon E}$ and $T_{\epsilon C}$ are the electron temperatures at the emitter and collector sides of the plasma, Σ_1 and Σ_2 are the macroscopic scattering cross sections of cesium and the inert gas respectively, ϕ_E and ϕ_C are emitter and collector work functions and V_C is the collector sheath height.

To facilitate comparison with experimental data, equation (1) can be written as,

$$\frac{1}{J} = \frac{1}{J_s} + K \exp \left(\frac{eV}{kT_{\epsilon E}} \right) \left[L + \frac{3}{4} P_1 P_{c1} d + \frac{3}{4} P_2 P_{c2} d \right] \tag{4}$$

where P_1 and P_2 are the pressures and P_{c1} and P_{c2} are the collision probabilities of cesium and the inert gas respectively.

According to equation 4, a plot of inverse current as a function of inter-electrode spacing should yield a straight line for each output voltage V.

C.   EXPERIMENTAL APPROACH

The gas injection system has been described in detail in the First Quarterly Report[IV-2]. It consists of several bakable expansion chambers and pressure regulating valves. The argon used in these experiments is the highest purity research grade commercially available. Before injection into the diode, the gas is passed through a liquid nitrogen trap to remove condensable impurities.

During the course of these experiments, it was noticed however, that in spite of all these precautions, the electron emission was increased by several orders of magnitude when argon was introduced in the system. This was traced to the presence of a residual oxygen pressure of the order of 10^{-8} torr. It is clear that this pressure of oxygen will result if the oxygen impurity in the argon is more than one part per billion at 100 torr of argon pressure.

To minimize its oxygen content, the argon was kept in a trap containing a mixture of zirconium and titanium chips at 400°C for about one hour. This technique was successful as indicated by work function measurements. A further modification was made in the cesium reservoir to allow full control over argon pressure while the diode is operating. Several sets of variable spacing families were obtained, subsequent to the incorporation of these improvements.

D. EXPERIMENTAL RESULTS

The data obtained cover a cesium temperature range of 533 to 553°K at the emitter temperatures of 1675 and 1800°K and 50 torr of argon pressure. A typical sample of variable spacing families is shown in Figure IV-1. The inverse electron current at constant voltage is plotted as a function of interelectrode spacing according to equation (4) in Figure IV-2. Note that constant voltage lines converge to a focal point whose coordinates, according to equation 4, are given by

$$\left[\frac{1}{J} \right]_o = \frac{1}{J_s} \tag{5}$$

and

$$[d]_o = - \frac{4L}{3(\rho_1 P_{c1} + \rho_2 P_{c2})} \tag{6}$$

Two other examples of variable spacing families, plotted in Figures IV-3 and IV-4, show such focal points.

A comparison of Figures IV-2, IV-3 and IV-4 shows that the abcissa of the focal points decreases with increasing cesium pressure. This is consistant with equation 6. To examine this dependence further, equation 6 is rearranged in the form:

$$\frac{1}{[d]_o} = -\frac{3}{4L} \rho_1 P_{c1} - \frac{3}{4L} \rho_2 P_{c2} \tag{7}$$

which shows that the $\frac{1}{[d]_o}$ should be a linear function of cesium pressure ρ_1. In the absence of inert gases equation (7) shows that a plot of $\frac{1}{[d_o]}$ versus ρ_1 should be a straight line passing through the origin. The slope of this line from the previous work[2] on electron scattering is expected to be approximately equal to $\frac{1}{14}$ (mil-torr)$^{-1}$. This dependence is represented as the dashed line in Figure IV-5. The abscissas of the variable spacing families in Figures IV-2, IV-3 and IV-4 are also plotted for comparison.

A comparison of equation (7) and Figure IV-5 shows that the fraction of electrons scattered by 50 torr of argon is much smaller than that scattered by 1 torr of cesium.

The implications of this result are that (a) The hypothesis that the saturation portion of ignited mode characteristics is diffusion dominated, is valid and (b) The inert gas atoms are essentially transparent to electrons of energies encountered in the ignited mode plasma and, therefore, potentially useful as ion diffusion barriers.

IV-4
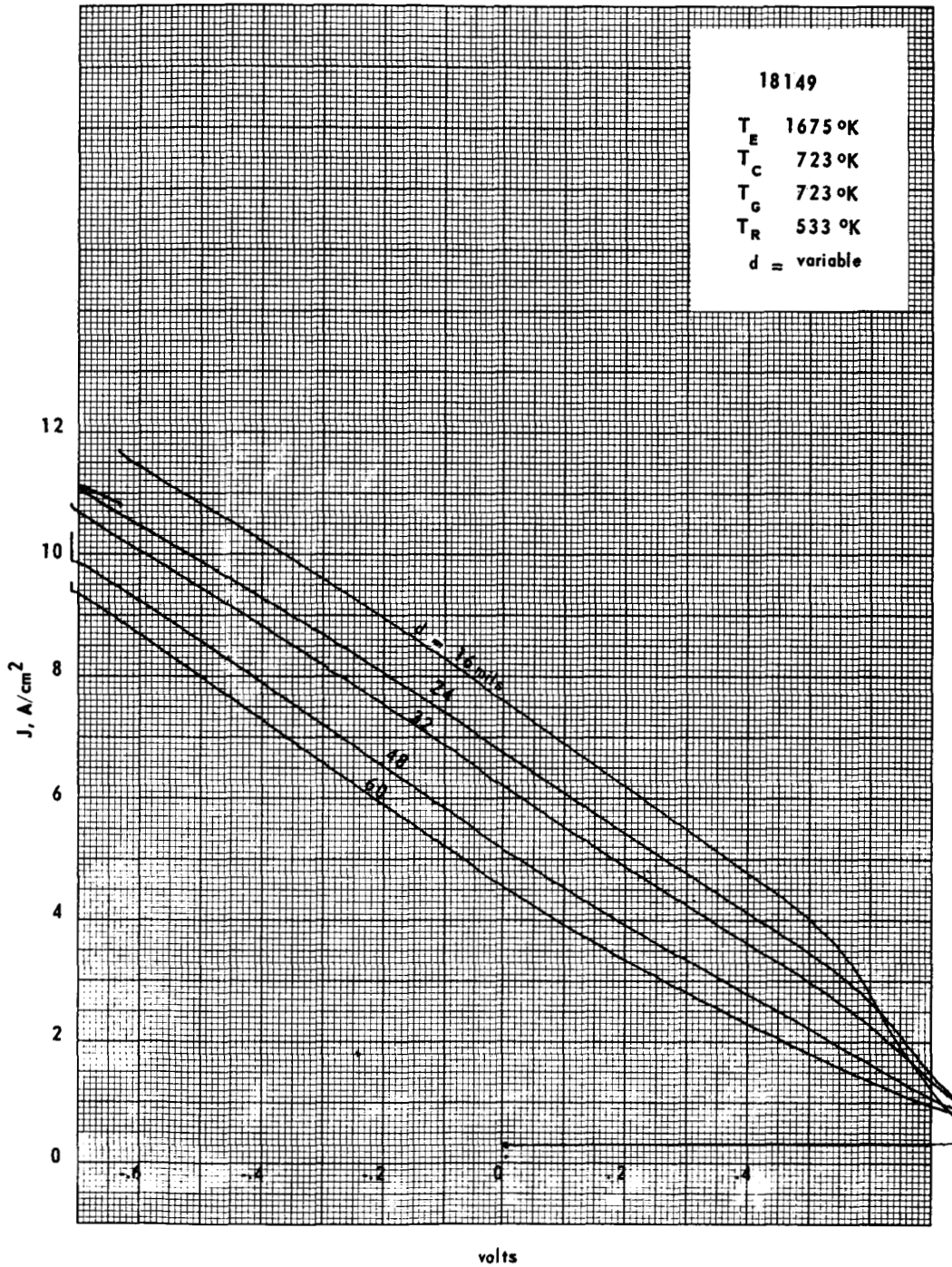
Figure IV-1. Typical Variable Spacing Volt Ampere Characteristics.
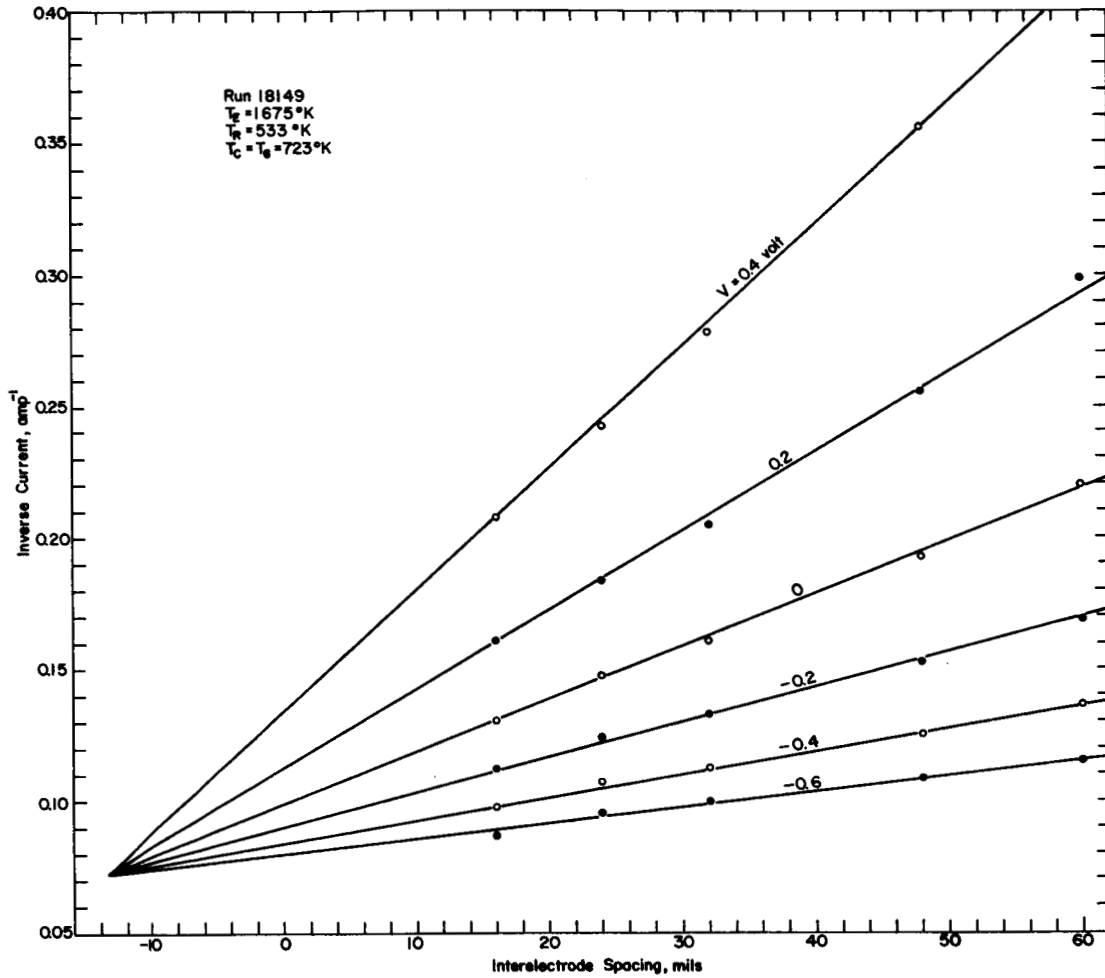
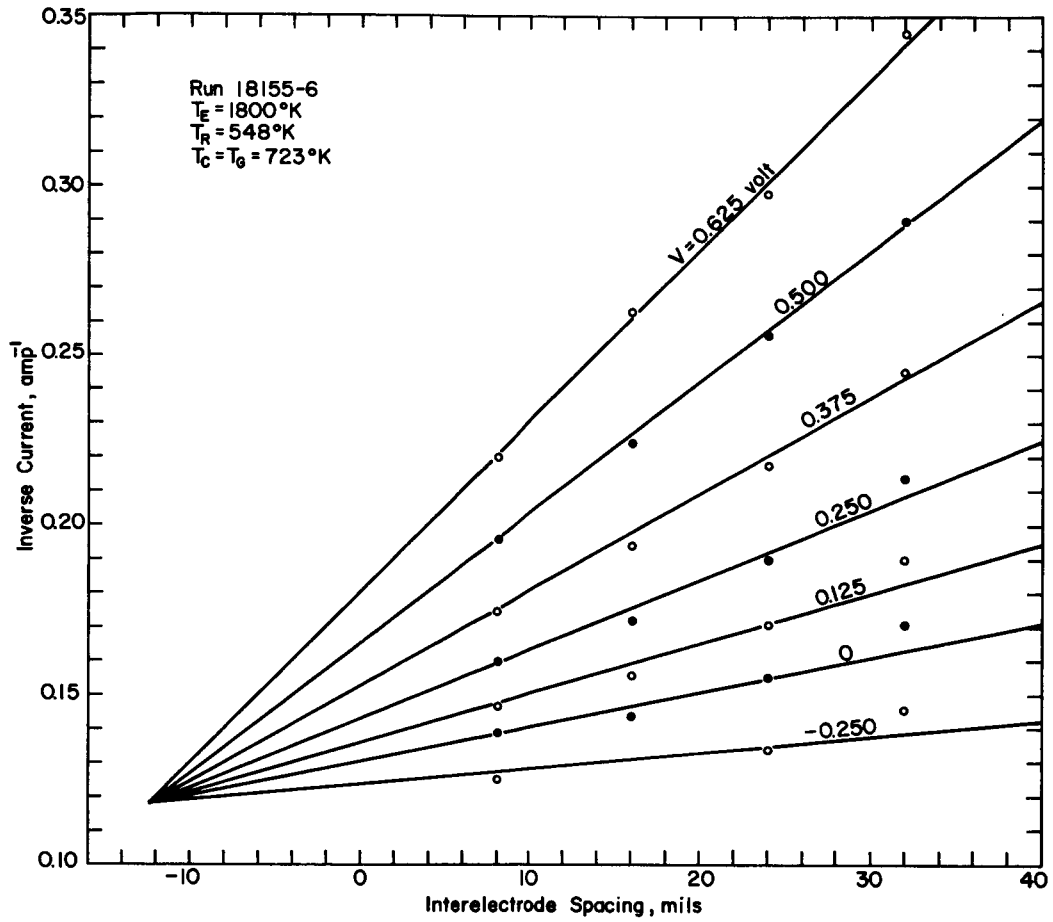Figure IV-2. Plot of Variable Spacing Families According to Equation 4.

Figure IV-3. Plot of Variable Spacing Families According to
Equation 4.

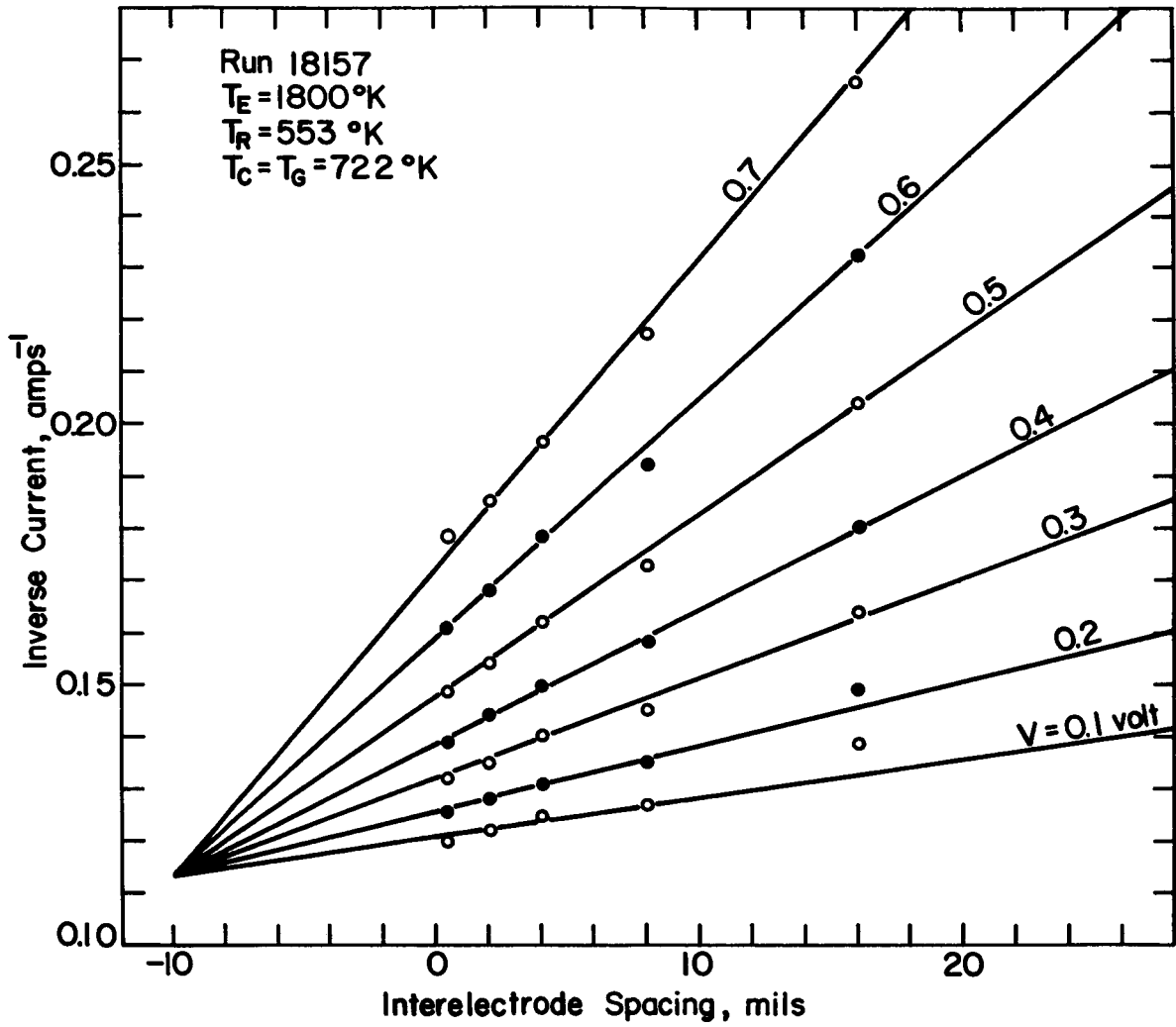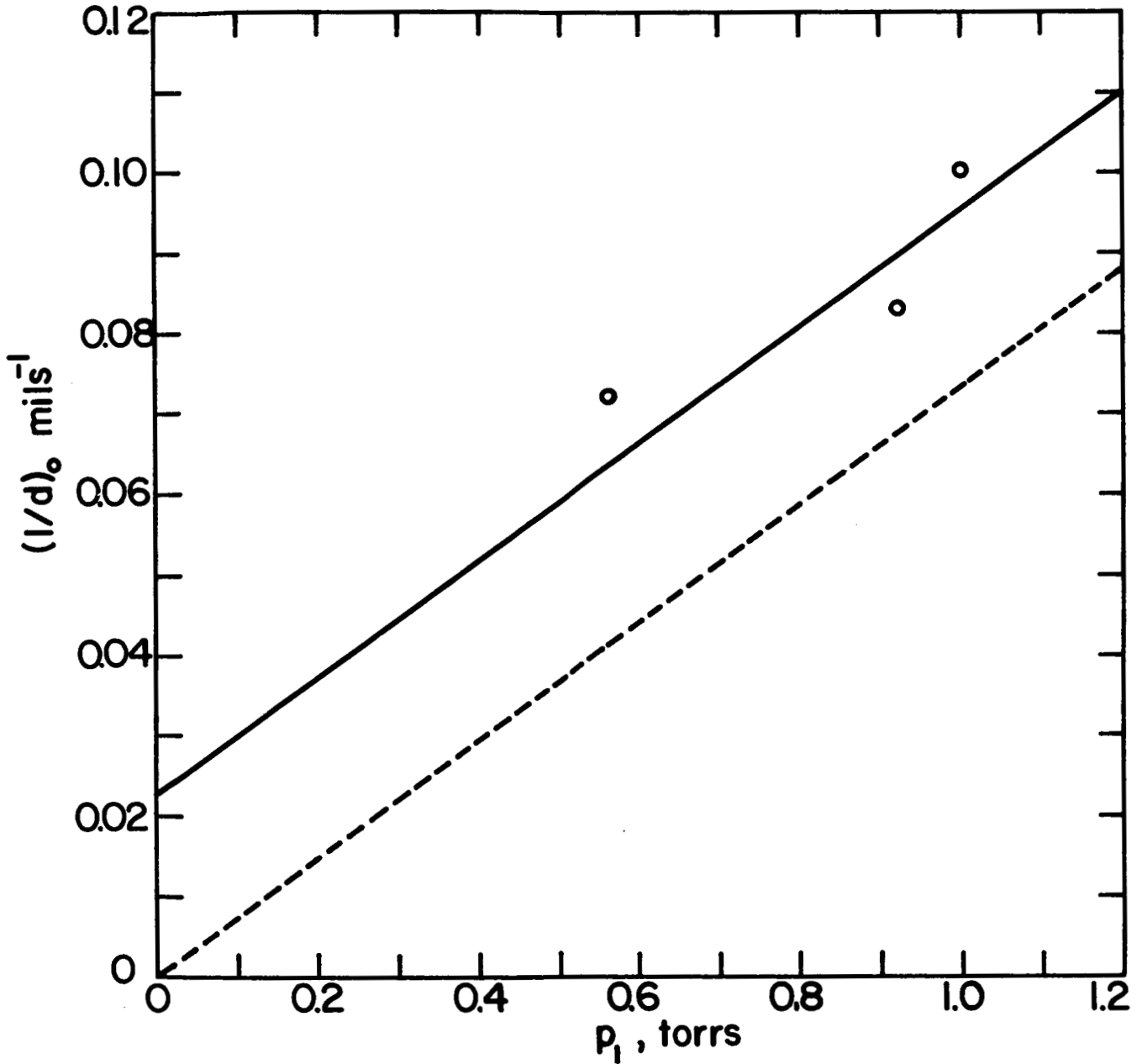Figure IV-4. Plot of Variable Spacing Families According to Equation 4.

Figure IV-5. Plot of the Focal Points in Figures 2, 3 and 4
According to Equation 7.

E. PARAMETRIC PERFORMANCE DATA

The rhenium emitter used in this task has an electroetched and heat treated surface. Its preparation and metallurgical examination were discussed in the First Quarterly Report[IV-2] of this program. The same report contained the results of bare work function and cesiated work function measurements. At the time note was made of the fact that the bare work function value of 4.88 eV was higher than that recorded for electropolished rhenium by 130 mV. Cesiated work function values were accordingly lower indicating that the etched rhenium adsorbed cesium more strongly and consequently would require less cesium more strongly and consequently would require less cesium pressure to achieve a given emission all other things being equal.

During the third quarter, the parametric performance study of this emitter material was completed. Families of current-voltage characteristics were generated by varying the cesium reservoir temperature, the collector temperature, the emitter temperature and interelectrode spacing. One hundred twenty five families representing about 1000 individual J-V curves were required to complete the study.

The performance of the device has been summarized using the envelopes of the variable cesium reservoir temperature families. Figures IV-6 to IV-10 show this summary. In each figure, the envelopes of several families taken at different interelectrode spacings but the same emitter and collector temperature are plotted. The collector temperature indicated was selected near the optimum value corresponding to the emitter temperature used. The dashed line in these figures represents the envelope of the spacing envelopes corrected for the emitter lead voltage loss. It corresponds to the output at the electrodes under fully optimized conditions for the emitter temperature indicated.

IV-10

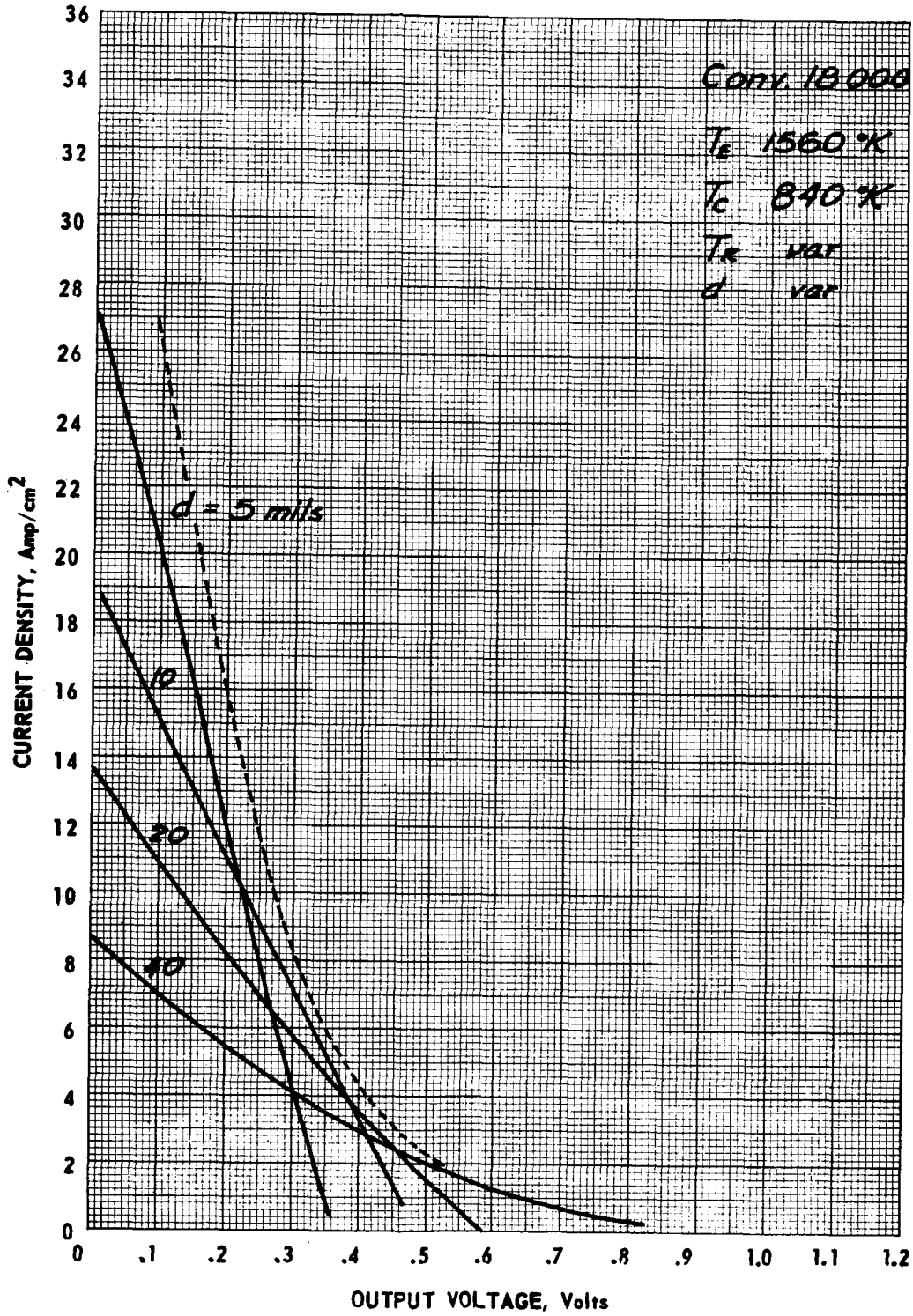Figure IV-6. Summary of J-V Families at 1560°K.

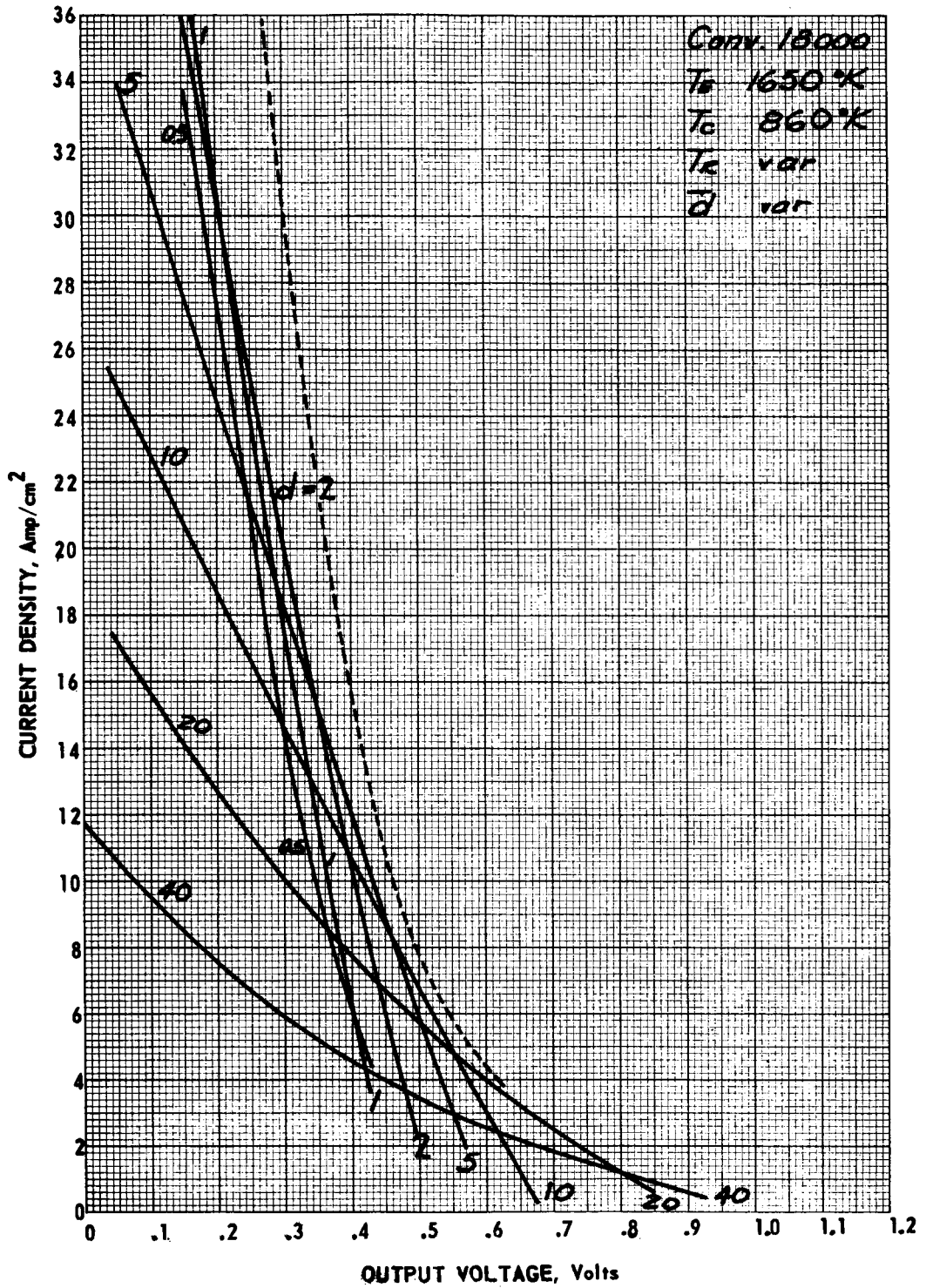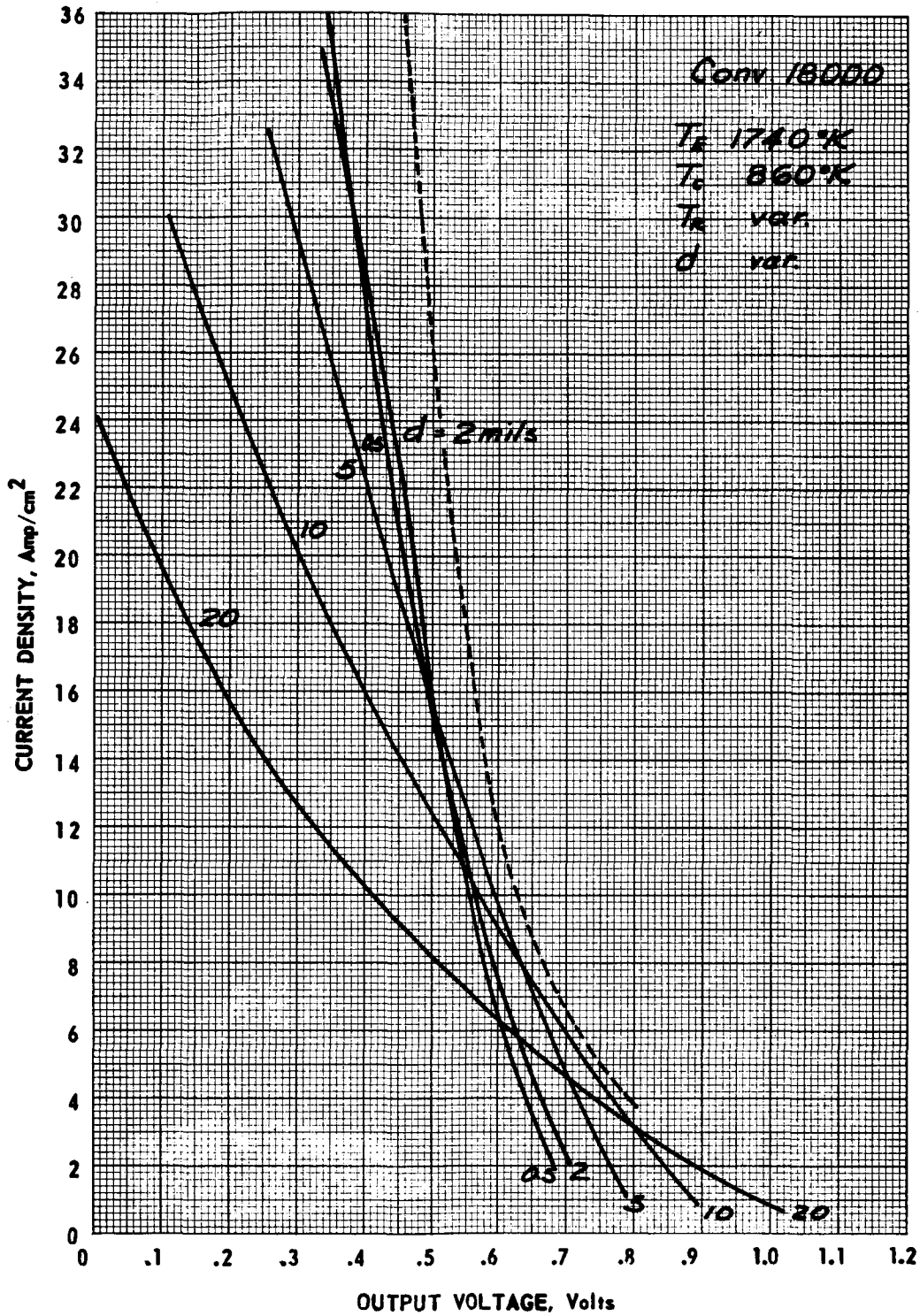Figure IV-7. Summary of J-V Families at 1650°K.

Figure IV-8. Summary of J-V Families at 1740°K.
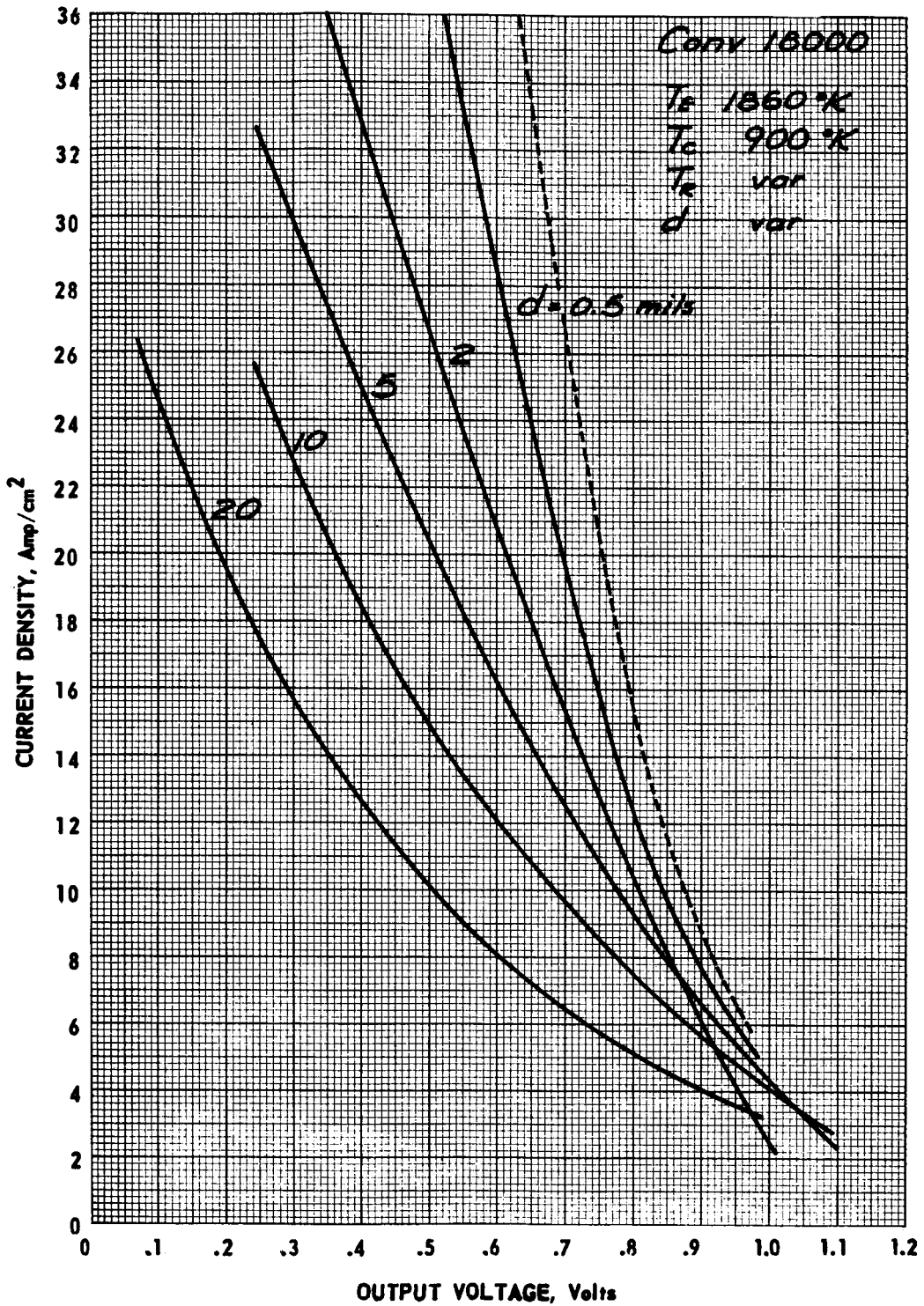
Figure IV-9.   Summary of J-V Families at 1860°K.
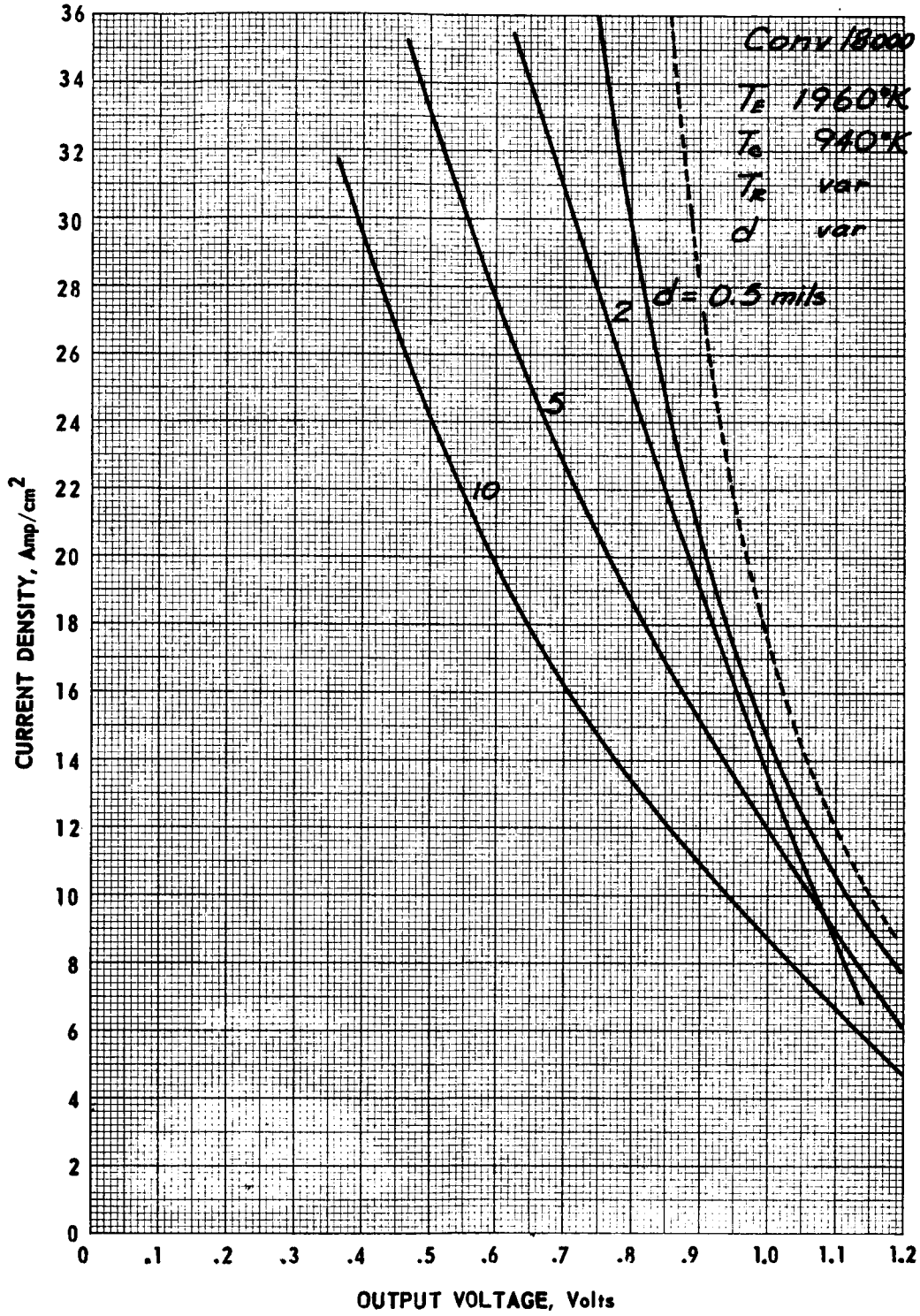
Figure IV-10.   Summary of J-V Families at 1960°K.

The fully optimized performance has been summarized in Figure IV-11 and the fully optimized electrode power output is shown in Figure IV-12. Comparison of Figure IV-12 with the corresponding figure for electropolished rhenium of Ref. IV-3 indicates that the etched rhenium has shown substantial improvement. This performance improvement is equivalent to an increase in spacing by a factor of 2.

REFERENCES

IV-1.   Kitrilakis, S.S. et al. ; Second Quarterly Progress Report for the Applied Thermionic Research Program (25 September to 25 December, 1965), Contract No. 951262; prepared for the Jet Propulsion Laboratory, Pasadena, California; Report No. TE 54-66.

IV-2.   Kitrilakis, S.S. et al. ; First Quarterly Progress Report for the Applied Thermionic Research Program (25 June to 25 September 1965), Contract No. 951262; prepared for the Jet Propulsion Laboratory, Pasadena, California; Report No. TE 23-66.

IV-3.   Kitrilakis, S.S. et al. ; Final Report for the Thermionic Research Program, Task IV, (2 August 1965), Contract No. 950671; prepared for the Jet Propulsion Laboratory, Pasadena, California; Report No. TE 7-66.

Figure IV-11. Fully Optimized Performance Map.
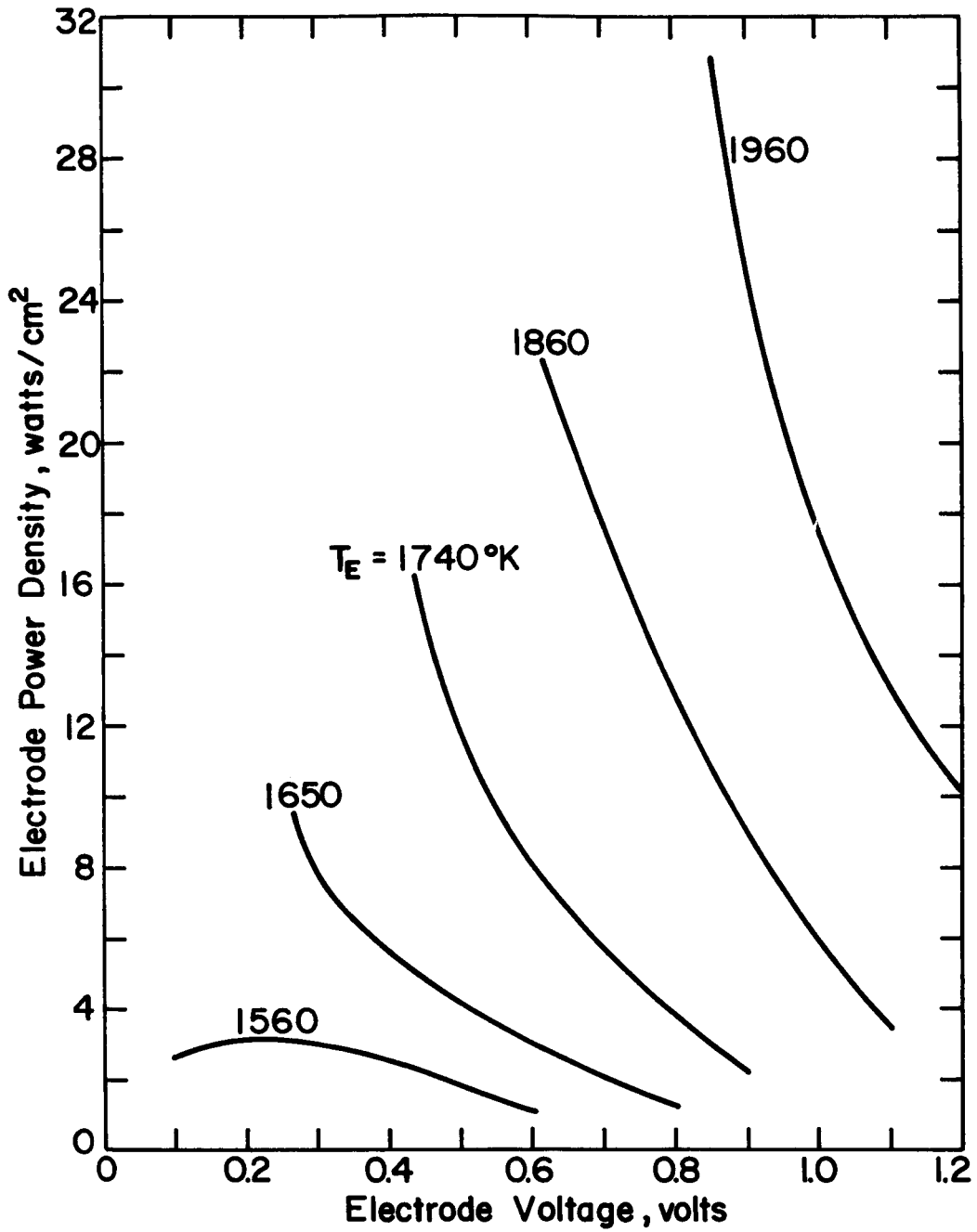
Figure IV-12. Fully Optimized Electrode Power Output Map.

APPENDIX A

LITERATURE REFERENCES TO WORK FUNCTION
MEASUREMENTS WITH FLUORINE COVERAGE

A literature search uncovered five references to refractory metal work function measurements in the presence of either free fluorine gas or CsF. These references have been abstrac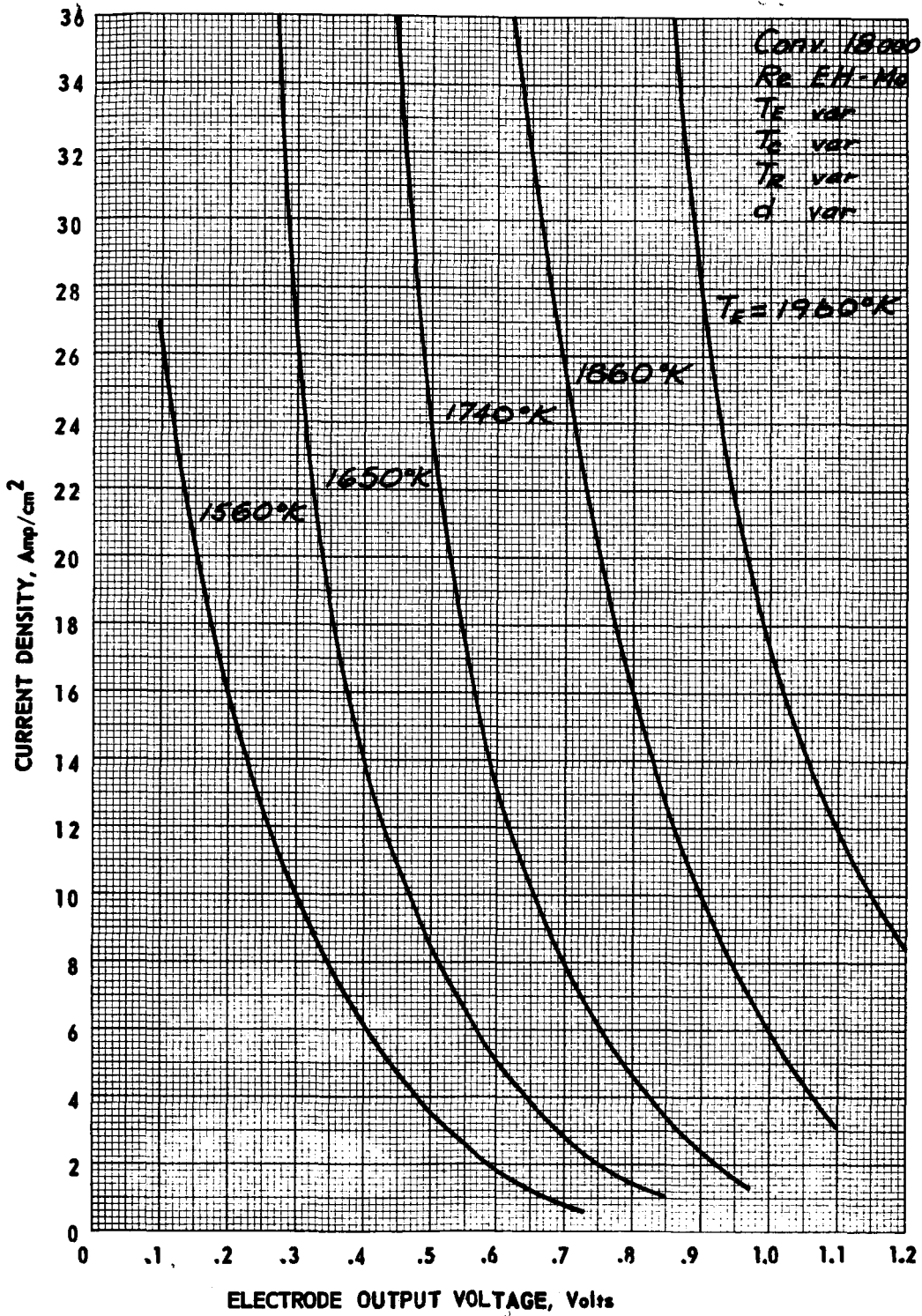ted in tabular form in Table A-1 and will be discussed here. The technical aspects of these investigations, will be examined in chronological sequence and the relative influence they appear to have had on each other will be pointed out.

Metlay and Kimball were concerned with the measurement of the electron affinity of fluorine. In this they were not successful, for reasons that are of no interest here, but in the process of measuring the ion and electron emission from a hot tungsten filament they observed an increase in work function which persisted to temperatures of 2600°K. They attributed this change to a tenaciously held adsorbed fluorine layer. They also experienced a rapid loss of tungsten which they explained by a peculiar dislodging action of fluorine atoms on the array of tungsten atoms ignoring the fact that tungsten fluoride cannot exist at these temperatures. Furthermore, having stated that this tungsten loss rate was unaffected by filament temperature and fluorine pressure, they went on to ignore completely the possibility of a third agent being responsible for the reaction taking place on the tungsten.

In general their technique was not what has come to be referred to as "vacuum technique" but rather one usually associated with chemical reaction vessels. The difficulties experienced by the authors are best explained by a

0.2 to 1% of oxygen contamination in the fluorine gas. This corresponds to 10^{-5} torr partial pressure of O_2. Part of this oxygen may have been contained in fluorine used, but it may have very well been released from the reaction of the pyrex wall of the vessel with the fluorine.

This work, nevertheless, was probably responsible for all subsequent halide investigations except for the work of Morgulis which was published in 1956.

Morgulis measured the work function of tungsten coated with CsCl versus CsCl coverage at 600 °C using the contact potential method. He measured coverage by using Cs tagged with Cs^{134} which he could count very accurately. The vacuum technique employed in this experiment was carefully controlled and as a result, the ultimate pressure in the device was 10^{-9} to 10^{-10} torr. The CsCl was found to lower the work function of tungsten by a maximum amount of 1.8 eV. The authors do not exclude the possibility of a "slight dissociation of the CsCl", but think it improbable. It is therefore questionable that their results are valid to thermionic emitter temperatures where complete dissociation is expected.

Aamodt and his co-workers, probably encouraged by Metlay's results, used CsF crystals as the source of fluorine. The maximum work function change (0.6 eV) and the desorption rates he observed are very much like those reported for O_2 by many workers and discussed elsewhere in this report. Ranken continued this work in a metal-ceramic tube, which, of course, avoids the difficulty of water evolution from the pyrex walls at 300 °C, but did not outgass his CsF higher than 220 °C.

Chronologically, our program started experiments with CsF next but that work has been discussed in detail in the August '65 annual report and of course, in current reports so it will not be summarized in this table.

Jester, Langpape and Minor worked at first with glass tubes and subsequently with metal-ceramic tubes. They also observed maximum work function changes of the order of 0.6 eV in tubes which had residual gas pressures exceeding 10^{-7} torr. They made steady state measurements and observed that the "additive effect" was lost after prolonged testing.

The summary Table, AI, in conjunction with the results of this program strongly supports the conclusions drawn in the body of this report. Perhaps, the single most important factor responsible for the error made by all the investigators of adsorbed halide films, with the exception of Morgulis, is the preconception, shared by all, that fluorine ought to behave like oxygen only more so.

TABLE A-I

Reference	Tube Type Absorbate(s)	Outgassing of Additive	Outgassing of Tube	Character of Experiment	Maximum Work Function Change and Activation Energy	Remarks
Mellay and Kimball	Glass tube F	None	None	Filament exposed to "microns" of Fluorine gas emission measured after evacuation	$\Delta\phi \approx 1.0$ eV	No awareness of vacuum technique.
Morgulis	Glass tube Cs Cl	Not given	Several 25-30 hr. outgassings Residual $10^{-9}-10^{-10}$ torr	Isotope tracer of Cs Cl coverage. Contact potential ϕ measurements tungsten temp. 600°C	$\Delta\phi = -1.8$ eV	Extremely clean system. Results of limited value to thermionic emitters.
Aamodt et al JAP 33	Glass tube Cs CsF	450°C Several hours	450°C Several hours	Coating of filament by raising CsF to 300°C -Transient w.f. measurements	$\Delta\phi \cong 0.6$ eV $E^* \ 145 \ \dfrac{\text{k cal}}{\text{gr-atom}}$	$E^* = 145$ k cal/mol. very similar to O_2.
Ranken	Metal tube Cs CsF F	220°C	325°C	Steady state at wall temp 250°-300°C Emission measurement	$\Delta\phi \approx 0.55$ eV	CsF outgassing inadequate.
Jester and Minor	Glass tube CsF	Not given	Residual gas pressure $>10^{-7}$ torr	Work function by emission in CsF steady state	$\Delta\phi = 0.7$ eV	Additive effect observed with "CsF" pressure of 10^{-11} mm Hg.
Langpape and Minor	Glass tube Cs CsF	Not given	Residual gas pressure	Work function by emission in CsF and Cs + CsF -	$\Delta\phi \approx 0.6$ eV	Additive effect observed with "CsF" pressure of 10^{-11} mm Hg.

APPENDIX B

CONVERTER EXPERIMENTS

Table B-I summarizes the converter experiments performed with CsF additive. All devices used a tungsten emitter and molybdenum collector and were similarly constructed. The emitter treatment in each case was an electropolish followed by annealing for about an hour at 2300°C. The second column shows the weight of CsF charge used and its outgassing time and temperature. Under $\Delta \phi_{max}$ is indicated the greatest change in work function observed during the experiments. The duration of this change is seen to be greater in the more poorly outgassed and uncesiated devices, again reenforcing the conclusion that the effects observed are due to oxygen contributed by the fluoride and gettered by the cesium in the CsF and Cs devices to make the effect disappear more rapidly.

GLASS TUBE EXPERIMENTS

Table B-II summarizes the glass tube results. In the first column are shown the tube number, filament material and relative length, and type of additive. Outgassing temperature and time for the envelope and additive are indicated, in some cases with the ultimate pressure at the pump. Note that this is not the tube pressure because of the tubulation conductance. The bare ϕ values are indicated where data could be taken; in several devices a stable bare value could not be obtained until after the envelope temperature (T_A) was raised. Apparently a layer of impurities was being stripped from the filaments. In each of the normally outgassed devices the maximum work function change observed was on the order of 0.7 eV. The specially dried fluoride sample showed a smaller $\Delta \phi$ max.

All the devices failed due to tungsten deposits on the walls making observation of the filament temperatures impossible. Rapid chemical attack also prevented testing with the Rhenium filaments.

These results are again consistent with the presence of large amounts of water vapor in the devices. Dissociation of the water at the hot filament to form tungsten oxide and hydrogen is thermodynamically favorable and the volatile oxide will then reach the cold walls where it will be reduced by the hydrogen. Thus, small amounts of water may transport a large quantity of tungsten. This is the water cycle described by Langmuir[*]. The oxygen is also available as an additive and fully accounts for all of the effects observed. The $\Delta \phi_{max}$ of 0.7 eV is typical of data obtained with oxygen under these conditions while at these low envelope temperatures, fluoride or iodide cannot be expected to have any effect.

---

[*] Trans. Am. Inst. Elec. Eng 32, 1921 (1913)
J. Am. Chem. Soc. 38, 2221 (1966)

TABLE B-I.   METAL TUBE EXPERIMENTS AT TEECO

Tube # / Emitter #	Additive Outgassing	Type of Experiment	$\Delta\phi_{max}$	E^*	Duration	Remarks
W-4	200°C 1 hr 300°C 1 hr $P = 4 \times 10^{-7}$ 0.3 g CsF	CsF only - work function	0.7	$t_{1910} = 45$ min 27 min	~130 hrs	
1000 W-6	200°C 20 hrs 300°C 3 hrs 0.3 gr CsF	Cs+CsF never showed additive effect	—			Very reproducible with Cs pressure slightly higher than usual
3000 W-6	200°C 3 hrs 300°C 3 hrs 200°C 18 hrs 1.2 grs CsF	Cs+CsF effects appear at 300°C full effect 450°C for 30 hrs certain after dissap. up 500°C	0.55 (Cs)		~ 30 hrs	After disappearance same as above
5000 W-9	250-300 3 hrs 300 2 hrs 300 10 min 200 10 hrs 1.2 gr CsF $P = 3 \times 10^{-7}$	CsF only - work function	(.7) 0.6		80 hrs	Effect disap. never came back. Ion current measurements indicate arrival of CsF at 450°C. Detected Cs via S-curves. $T_R \approx$ room temperature. Cesiated and obtained same as 3000 and 1000 bare line ~<4.6

TABLE B-II. GLASS TUBE EXPERIMENTS AT TEECO

Tube # Emitter Material Charge	Outgassing Glass T, t Charge T, t	Experimental Work Function Results	Maximum Work Function Change Observed	Mode of Failure Remarks
9000 W, short filament CsF	400°C 3 hrs. 400°C 3 hrs. (in envelope)	ϕ bare ≈ 5.0 eV ϕ_{max} ≈ 5.7 eV at 195°C ϕ vs T_A shows max.	~0.7 eV	Fil. disappeared rapidly at 300°C. Visible W deposits on glass. Photo of fil. Figure I-10
11,000 W, long filament CsF	400°C 3 hrs.	ϕ bare ≈ 4.8 eV ϕ_{max} ≈ 5.4 eV at T_A 80 - 200°C	~0.7 eV	Fil. disappeared rapidly at 300°C. W deposit on glass.
12,000 Re, W long filament CsI	300°C 3 hrs. 300°C 3 hrs. (in tubulation) 3×10^{-6} ultimate	Bare difficult to obtain ≈ 5.2 eV at start. Later 4.7 eV ϕ_{max} ≈ 5.4 at T_A 150°C	~0.7 eV	Fil. disappeared at 350°C Re not used. Highly contaminated. Bare ϕ_e stabilized only after envelope was cycled to 200°C with 1600°C Te
13,000 Re, W long filament Control	300°C 3 hrs. 3×10^{-6} ultimate	Like 12,000, ϕ_{bare} ≈ 4.7 eV ϕ_{max} ≈ 5.4 eV at T_A 100°C	~0.7 eV	Stopped for re-outgas Fil. started to disappear
14,000 Re, w long filament CsF Special drying	400°C 100 hrs. 1×10^{-6} ultimate 500°C 1 hr. 600°C min.	ϕ_{bare} ≈ 4.75 eV ϕ_{max} ≈ 5.0 eV at 240°C T_A With T_A ≈ 240°C Re filament was heated	~0.25 eV	W glass deposit Best control slow coating of glass. Least effect on ϕ Re fil. rapidly attacked
15,000 Re, W, long filament Control	400°C 100 hrs. 5×10^{-7} 300°C 50 hrs. 5×10^{-7}	Unstable		W fil. attacked. Unstable ϕ_e with slow drifting